The Combined Effect of Waste Glass Sand and Glass Fiber on the Improvement of Thermal Property of Aerated Concrete

Inzhu Yerbolat, B.Eng

Submitted in fulfilment of the requirements for the degree of Masters of Science in Civil & Environmental Engineering

School of Engineering and Digital Sciences

Department of Civil & Environmental Engineering

Nazarbayev University

53 Kabanbay Batyr Avenue,

Nur-Sultan, Kazakhstan, 010000

Supervisors: Chang-Seon Shon

April 2021

Declaration

I hereby, declare that this manuscript, entitled “The Combined Effect of Waste Glass Sand and Glass Fiber on the Improvement of Thermal Property of Aerated Concrete,” is the result of my own work except for quotations and citations, which have been duly acknowledged. I also declare that, to the best of my knowledge and belief, it has not been previously or concurrently submitted, in whole or in part, for any other degree or diploma at Nazarbayev University or any other national or international institution.

Name: Inzhu Yerbolat

Date: 11.04.2021

Abstract

Aerated concrete (AC) is a lightweight, energy-efficient, and non-combustible material comprised of cement, lime, gypsum, aluminum powder, water, and silica-rich materials such as sand and fly ash. The AC has the characteristics of lower density, compressive strength, and thermal conductivity due to its high porosity. This thesis work investigates the thermal, mechanical, and physical properties of none-autoclaved aerated concrete (NAAC) partially containing waste soda-lime glass sand and glass fiber. The use of waste glass and glass fiber can eliminate the autoclaved curing process by enhancing the physical and mechanical properties in AC and approach sustainable use of waste glass as an alternative construction material. The mixture parameters included the partial substitutions of normal sand with soda-lime glass sand (15% and 30%) and glass fiber (1%, 2%, and 3%) and included the replacement of cement with 30% fly ash. The fly ash was substituted to prevent the concrete cracking due to the alkali-silica reaction between the cementitious materials and waste glass aggregate. A series of tests were conducted to determine the density, absorption, porosity, and compressive and tensile strengths of the NAAC. Test results indicated that density, porosity, and strength have a strong relationship with each other. Furthermore, it was determined that the increase of glass aggregate content leads to decreasing the thermal conductivity while the increase in glass fiber content results in increasing the thermal conductivity of the NAAC. However, the thermal conductivity of the NAAC mixture combined with soda-lime glass sand and glass fiber was lower than that of the NAAC mixture containing normal sand. Moreover, test results show that the increase of glass sand content leads to increasing both compressive and flexural strengths. Furthermore, the combined use of glass sand glass fiber also increases the strength up to 2 times. Finally, the optimized mixture proportion was applicable to predict the thermal conductivity equation with reasonable accuracy based on the multiple linear regression method with Minitab Software. Also, the energy conservation of NAAC was analyzed by Design Builder software. The results indicated that the NAAC has the lowest heating and cooling loads, minimum site and source energy than other conventional materials used in Kazakhstan.

Acknowledgements

I would like to express my sincere gratitude towards my thesis supervisor Assistant Professor Chang-Seon Shon of the Civil and Environmental Engineering Department at Nazarbayev University. Professor Shon constantly supported, contributed, encouraged, and helped me to coordinate this thesis work. His effort, deep knowledge, and academic ethic promoted my successful work under this project.

I also uppermost gratitude to a first-year graduate student at Nazarbayev University Kirill Kryzhanovskiy and alumnus of Nazarbayev University Aidyn Tugelbayev, Ramazan Shaimakhanov, and Nariman Karatay for their significant contribution by helping me in laboratory works.

Also, I give my special thanks to all the Civil and Environmental Engineering Department professors for their valuable suggestions, which were given during the project work.

Additional acknowledgment is for NPO Young Researchers Alliance and Nazarbayev University Corporate Fund "Social Development Fund," where I won the grant under their Fostering Research and Innovation Potential Program. For their funding, I bought laboratory consumables, published a conference paper, and participated in an international conference, where I expanded my knowledge about this project

Table of Contents

List of Figures

List of Tables

Chapter 1 - Introduction.

1.1 Background

Aerated concrete (AC) is a lightweight, energy-efficient, excellent thermal insulative, and fire-resistant material. It is mainly made of cement, lime, gypsum, aluminum powder, sand, water, and silica-rich materials such as fly ash [1]. The AC has many advantages in terms of structure, properties, and usage. The prominent privilege is its lightweight, which leads to the reduction of supporting loads. Therefore an excellent economy can be succeeded in the design and construction of foundation and reinforcement [1, 2]. Another benefit of aerated concrete is its excellent thermal property due to the millions of evenly distributed air voids [1 - 3]. High thermal insulative material in building construction leads to the reduction of energy consumption and operation payment for heating/cooling. Moreover, the unique characterization of AC is high porosity. The porosity of AC can be varied from 75% to 90%, and it depends on the composition and method of curing [1, 4]. All properties of aerated concrete, such as thermal conductivity, strength, shrinkage, and permeability, mainly depend on porosity and pore size distribution. Also, AC's unit weight is between 300 - 600 kg/m^3, making it approximately four times lighter than normal concrete. Since Aerated Concrete is lightweight, and its density can vary from 300 to 1800 kg/m3, it is flexible and easy to use in different applications [2].

Despite the AC's excellent thermal performance, both the compressive and tensile strengths of the AC are relatively low because of its low density and high porosity. However, if glass fiber and strength-enhancing material are used in AC production, both compressive and tensile strengths can be improved.

There are two types of aerated concretes, which differ from each other by the curing method. They are none-autoclaved aerated concrete (NAAC) and autoclaved aerated concrete (ACC). The curing process and duration mainly affect to properties of this material. The normal curing process is used in the production of NAAC, while AAC is produced by curing under some pressure [1]. Because of the production under pressure, AAC's strength will be higher up to 20% than the NAAC. On the other hand, the autoclaving process has a potential risk to the environment and economy because of the high pressure and temperature operation processes. Therefore, the NAAC was cast in this thesis work. Moreover, the strength-enhancing material glass fiber will be used to produce NAAC to improve the mechanical properties.

1.2 Problem statement

According to the literature review, every year, 200 million tons of glasses have been disposed to the landfill in the world. Moreover, 80% of waste glasses contain soda-lime glass type [5]. The soda-lime glass is a widely prevalent glass, which is used for bottles, jars, and window panels [6]. Kazakhstan is also facing the problem of disposing of waste glass and its recycling. 340 thousand tons of waste glasses are accumulated every year, and 30 thousand tons of them are recycled. It means that because only 8.8% of glasses per year are recycled and reused, the remaining 91.2% of waste glasses are disposed to landfills in Kazakhstan [7]. Therefore, it is necessary to find appropreate approaches to utilizing waste glasses in construction applications, especially in materials preparation.

Another challenge facing our world nowadays is the increase in energy demand and consumption. Kazakhstan is one of the coldest countries, so long-lasting winter and cold days contribute to high energy consumption for heating. Also, it leads to high expense for heating. Moreover, more than 30% of energy is consumed by residential buildings in Kazakhstan [8]. Therefore, the residential buildings should construct with excellent thermal insulative material, like Aerated Concrete.

1.3 Research Objectives and Scopes

This study's main objective is to evaluate the combined effect of waste glass sand and glass fiber on the improvement of thermal properties of non-autoclaved aerated concrete (NAAC). This was achieved by developing a robust and reliable test protocol that can assess the NAAC’s thermal properties. Major topics to solve the earlier mentioned problem statements covered in this thesis are summarized as the following:

- Development of mixture proportions of NAAC consisting of combined waste glass sand and glass fiber to improve the thermal performance
- Development of integrated test methodologies to evaluate physical and mechanical properties of NAAC
- Evaluation of the combined effect of waste soda-lime glass sand and glass fiber on improving the thermal properties of NAAC
- Development of a statistical model to predict the thermal conductivity of NAAC
- Analysis of a simulation model that applies the developed NAAC to residential buildings in Kazakhstan

1.4 Thesis structure

This thesis consists of five chapters, each with specific objectives. The first introduction chapter gives background information, problem statement, research objective and scopes, and the thesis's overall structure.

The second literature review chapter focuses on the published articles about the properties of none-autoclaved aerated concrete and their testing methods. This part's vital issue is to identify the main characteristics that affect the thermal performance of NAAC and their mixture proportions. Moreover, this part includes the recent work of researchers who have used waste glasses or glass fibers to prepare construction materials, especially in concrete. Furthermore, the various models and software, which can predict the thermal conductivity equation, analyze the energy performance, and feasibility of NAAC are reviewed in this chapter.

The third chapter is the experimental program, which includes four main sections. The first one is to determine the basic characterization of materials, such as particle size distribution, mineralogy using X-ray diffraction, sieve analysis, chemical composition, and aggregate properties. All experimental procedures have been done based on the ASTM Specifications. The second section is to optimize the mixture proportion of NAAC. The mixtures' main parameters are the content of normal sand, waste glass sand, glass fiber, cement, and fly ash. The statistical software Minitab has been used to determine the mixture proportion of NAAC, yielding the material's optimum thermal characteristics. The third section of the experimental program in this chapter is the sample preparation. The complete information about the specimen preparation procedure is also given in this chapter. The final part of this section is to conduct various tests to evaluate the properties of NAAS samples. It should be noted that four samples have been tested for each property testing, and then the average of specimens has been taken for analysis.

Chapter 4 is the most important part of the thesis, including analyzing all obtained test results. In this chapter, the relationship between the physical and mechanical properties of NAAC, the relationship between mixture parameters of NAAC and thermal conductivity, and the relationship between physical properties of NAAC and thermal conductivity have been analyzed.

In chapter 5, the evaluation of energy conservation, a statistical prediction model of thermal conductivity, and the feasibility of NAAC have been discussed.

Finally, the summary of main findings and recommendations are reported in Chapter 6.

Chapter 2. Literature Review

In recent years, several types of research were conducted to evaluate aerated concrete (AC) and non-autoclaved aerated concrete (NAAC) in terms of its types, properties, and production methods. This chapter summarizes the previous studies conducted by other researchers. Firstly, a general overview of AC is presented. Then, the accumulation of waste glasses, their effect on the environment, and their application in construction areas are discussed. Then, the effect of waste glasses on the thermal and mechanical properties of aerated concrete is analyzed. Moreover, this chapter includes the studies about the 'DesignBuilder' software and 'Minitab' statistical software, which is used to evaluate energy saving effect and model the prediction equation for the thermal conductivity of none-autoclaved aerated concrete, respectively.

2.1 Aerated Concrete and Non–Autoclaved Aerated Concrete

Aerated concrete (AC) is one of the types of lightweight concretes globally used because it is a lightweight and energy-efficient construction material, which provides excellent thermal insulation and fire resistance [1]. The AC can be considered an environmentally friendly and green product because it is mainly made from sand, lime, gypsum, cement, aluminum powder, water, and silica-rich materials that come from industrial by-products such as fly ash, ground granulate blast furnace slag, silica fume, etc. [9]. The composition and mixture proportion of AC can be varied depending on its application and work scope. According to studies, 33% and 67% of AC's total mass contains water and solid components, respectively. Moreover, from solid components proportion, 59% contains fine aggregates, 33% contains cement and gypsum, 8% contains lime, and 0.07% contains aluminum powder [1-4]. However, this mixture proportion is not unique and can be differ based on the purpose of use. Moreover, Coradini [10] claims that AC component materials and wastes can be recycled and reused, which confirms this material's environmental aspect. Therefore, AC has many advantages in terms of structure, properties, and usage.

One of the essential characteristics of AC is its porous structure. According to Narayanan et al. [1], the porosity of AC is as high as 80%, and it depends on the composition and method of curing. The chemical reaction between the aluminum powder and water leads to the production of hydration gas. Then, this hydration gas is trapped in the concrete mixture and forms voids. All these processes have resulted in the aeration of material. The following Equation 2.1 shows the chemical reaction between aluminum powder, calcium hydroxide, and

water. As can be seen, after reaction, microscopic hydrogen-air bubbles is produced in the mortar and leads to the volume increase and generation of pores [4].

$$2Al + 3Ca(OH)_2 + 6H_2O \rightarrow 3CaO.Al_2O_3.6H_2O + 3H_2 \quad (2.1)$$

Aluminum powder + Hydrated Lime + Water → Tricalcium Hydrate + Hydrogen (2.2)

According to the studies, thermal conductivity, strength, shrinkage, and permeability properties of AC are mainly depend on porosity, volume expansion, and pore size distribution. For example, Hamad [2] claims that the less volume increase leads to the strength-enhancing. However, high volume expansion with more pores in the material leads to the decrease of the thermal conductivity value, which results in better thermal performance of the material. Moreover, AC's unit weight is between 300 - 600 kg/m^3, which makes it approximately four times lighter than the normal concrete [1, 2]. Because of its lightweight characteristics, the supporting loads can be reduced, which results in a great economy in the design and construction of foundation and reinforcement.

As stated earlier, AC provides better thermal insulation, conserves temperature, reduces energy consumption, and reduces utility bills for heating the house. European Autoclaved Aerated Concrete Association claims that AC's thermal efficiency characteristic is 3 and 10 times better than the clay brick and normal concrete, respectively, because of its cellular structure [11].

Researchers have proved the energy efficiency quality of AC material. For example, Radhi [12] presented that using AC material in a building's wall layer can reduce energy consumption by 7%. Moreover, approximately 350 kg of CO_2 emissions can be saved by each $1m^2$ of AC wall throughout the building's life cycle [9]. According to the research survey conducted by the Portland Cement Association, 77% of professionals assert that the AC can be considered as a sustainable material, which corresponds to all requirements of sustainability [13].

Several research simulations were conducted to compare and analyze the different building materials in terms of energy consumption. For example, Kaska and Yumrutas [14] have compared blockbims , brick, briquette, and autoclaved aerated concrete (AAC), which are the most commonly used wall materials in Turkey. The simulation results indicated that less heat was gained while using AC and blockbims systems as an exterior wall. Also, Heathcote [15] conducted research based on determining the inside temperature of building

without air-conditioners during the summer days. Brick veneer, mud brick, and AAC materials were used to conduct this research. Simulation results demonstrated that the inside temperature of the building model used AAC was 26.5°C, while the temperature of the building simulated by brick veneer and mud-brick was 26.9°C and 27.6°C, respectively. According to the experiment conducted by the NCMA, the interior surface temperature of the 10-inch AC wall was the only 3°F, while the exterior surface wall temperature was 126°F. These tests showed that less amount of heat would be transferred through the wall made of AC, which leads to the reduction of energy consumption for cooling the house [13]. According to Aybek's research simulation, building models made with AC consumed 14% and 11.6% less energy than the wood-framed and metal-framed model, respectively, during the one year in Atlanta city [13].

The manufacturing and utilizing of AC products become popular all over the world. Research studies show that the AC has been used throughout the world in different climates. For example, AC is utilized in cold regions like northern Europe, in hot and humid regions as the Far East, in hot and dry regions like Australia [16]. Therefore, like in Nur-Sultan city, the temperature difference is no problem for buildings made of AC products because these buildings keep warmer during the winter and keep cooler during the summer season.

There are two types of aerated concrete: AAC and non-autoclaved aerated concrete (NAAC). They differ from each other by the production method [2]. As shown in Figure 2.1, AAC is mainly produced by using an autoclave curing, which is operated with high pressure and temperature. Thus, the production of AAC has a potential risk, and its cost is relatively high. Since the less amount of mixtures will be produced in this thesis scope, autoclave curing will be replaced with simple curing techniques, which is described clearly in the experimental program part (Chapter 3)

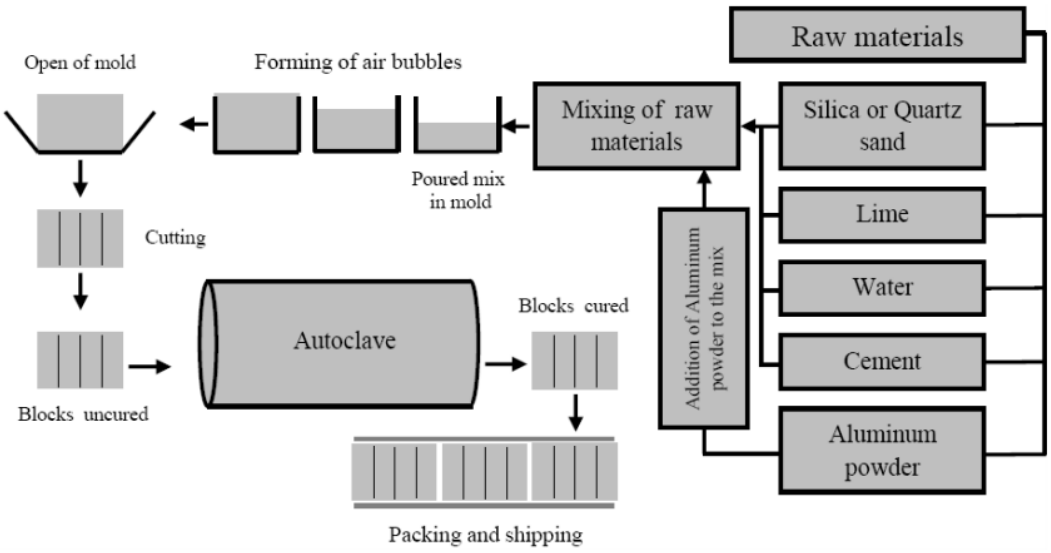

Figure 2.1 Process phases of AAC production [2]

2.2 Waste Soda-Lime Glass

Glass is a transparent and widely used material, which is produced by melting a mixture of silica, soda ash, and $CaCO_3$. Also, it is an ideal material for recycling and reusing for different applications. As stated earlier, the goal of thesis work is to analyze the effect of waste soda-lime glass sand and glass fiber on NAAC properties. According to the literature review, every year, 200 million tons of glasses have been landfilled globally. Moreover, 80% of waste glasses contain soda-lime glass type [5]. The soda-lime glass is a widely prevalent glass, which is used for bottles, jars, and window panels [6]. Kazakhstan is also facing the problem of disposing of waste glass and its recycling. About 340 thousand tons of waste glasses are accumulated every year, and 30 thousand tons of them are recycled. It means that only 8.8% of glasses per year are recycled and reused. The remaining 91.2% of waste glasses are disposed to landfills in Kazakhstan [7]. Therefore, it is necessary to find an emerging technology to use waste glasses in construction applications. Moreover, this leads to enhance sustainability in environmental and economic aspects.

In recent years, several types of research were conducted to evaluate the effect of waste glass on construction materials' property. For example, Liu et al. [17] reported that when the normal sand was partially replaced with glass aggregate, the thermal property of concrete using glass aggregate was improved by 32.9% more than concrete containing normal sand at 1000 kg/m^3 density. This property in lower density was more dominant than that in high density. They also found that smaller particle sizes of waste glasses (< 100μm) get better

results in decreasing concrete thermal conductivity value. An equivalent result was obtained by Liang et al. [18], which is that the waste glass material with a smaller size distribution leads to better thermal performance. They also found that the large percentage of recycled glass content with smaller pore size leads to the improved concrete thermal property.

On the other hand, Pehlivanlı et al. [19] investigated the effect of glass fiber on the thermal conductivity, compression, and flexural strength of autoclaved aerated concrete. They reported that glass fiber used as a quartz replacement leads to the 1% enhancement of all mentioned properties. Gautam et al. [20] analyzed the effect of waste glass on the compressive strength of concrete by replacing the normal sand with 10%, 20%, 30%, and 40% glass sand. They concluded that 10% and 20% replacement shows a significant increase in compressive strength at a 7 day, such as 47.75% and 13.64%, respectively. At 28-day, the compressive strength was increased by 3.30% and 2.18%, respectively. However, 30 % and 40% replacement leads to a minor decrease in compressive strength. Therefore, they summarized that 10% glass sand could be considered an optimum replacement in compressive strength enhancement [20]. Dong et al. [21] explained why the thermal conductivity of concrete made from glass sand is lower than that made from limestone. The production method is where the limestone absorbed more water than glass and because of the rehydration in limestone.

According to Chung et al. [22], modern building materials' characteristics are durability, minimum mechanical property, and energy-saving property. Therefore, thermal conductivity can be considered one of the important properties of materials. Many researchers evaluated and proved the favorable effect of waste glasses on the properties of concrete. For example, Yu et al. [23] stated that up to 40% replacement with waste glasses resulted in better thermal characteristics. Also, Alani et al. [24] explored the thermal conductivity decrease from 2.0 W/mK to 0.7 W/mK while using fine waste glass sand. The same results were obtained by Chung et al. [22] studies. They summarized that using the crushed waste glasses can produce lightweight concrete with a density lower than 2000 kg/m^3, with compressive strength of more than 36 MPa, and with thermal conductivity lower than 0.6 W/mK. It can be concluded that material made from crushed glass sand can fulfill all mechanical and thermal properties.

Some studies show the drawback effects of using the glasses as aggregate in concrete production. One of the important negative aspects is the alkali-silica reaction (ASR). Since

the cement contains a high-alkali pore solution and glass contains silica, their reaction can lead to concrete expansion and cracking [25]. Nevertheless, some researchers explored ways to eliminate the ASR problem by successfully optimizing the mixture proportion and replacing the cement with supplementary cementitious materials such as fly ash, ground granulated blast furnace slag, metakaolin, and others [22].

Therefore, if waste glass aggregate and glass fiber are used together, several synergetic effects are obtained. This thesis work investigates the thermal, mechanical, and physical properties of NAAC partially containing waste soda-lime glass sand and glass fiber to eliminate the autoclaved curing process to fit sustainable use of waste glass as an alternative construction material. The mixture parameters included the partial substitutions of normal sand with soda-lime glass sand (15% and 30%) and glass fiber (1%, 2%, and 3%) were examined on the properties of the NAAC.

2.3 DesignBuilder Software

This study investigates the energy conservation of 5-floor residential building made from NAAC materials. Since the various parameters affect to the energy performance of building, it is better to use the energy simulation tools, such as Design Builder. It is a powerful software, used to estimate the energy consumption of buildings, by considering all factors, such as design geometry, location, weather, climate changing, HVAC systems, lighting, occupancy, construction materials, etc. More specifically, this software calculates the heating load, cooling load, total site and source energy, embodied carbon, cost [33].

Several research simulations were conducted by Design Builder to analyze the energy consumption of buildings and to compare with actual values. For example, Eskin and Turkmen [34] analyzed the annual heating and cooling loads of office building in Turkey. They summarized that the difference with actual value of heating and cooling loads was 3% and 5%, respectively. Fathalian and Hadi [35] assessed the validation of Design Builder software, by comparing actual and simulated annual energy consumption of building in Iran. The difference was constituited less than 1.6%. They summarized that the minor differences might be because of the error in input data such as unspecified parameters. Choi et al. [36] also analyzed the thermal behaviour of multi-story double-skin facade building in South Korea, whereas Zomorodian and Tahsildoost [37] compared the actual results of heating and cooling loads of educational building in Iran with the simulation results. Their results also verified the accurate performance of Design Builder Software.

In a research conducted by Sadeghifam et al. [38], the effect of each building element, such as walls, floors, roofs, and ceilings on the energy saving of building in Kuala Lumpur were investigated. The wide range of materials were chosen for each element and the most optimized materials, which lead to the lowest energy consumption of building was selected by Design of Experiment (DOE) method. Moreover, they summarized that the ceiling materials, wall materials and temperature affected significantly on the energy performance. The research work of Pawar and Kanade [39], shows that the results obtained from the Design Builder software is more accurate than the other energy simulation tools.

In a research conducted by Cardenas et al [40], the energy performance of educational building in Columbia was analyzed by zones. They summarized that the zones with many occupants and temperature above 27°C are considered as the discomfort zones. In addition, the daylight level of the zones located in the upper floor is 33% growth because of the solar pipes. The energy consumption of zones with green roofs reduced till 5% than the other zones. Finally, the difference between the measured and simulated results was 4% and it validates that the DB is a powerful tool to estimate the energy analysis in a tropical environment.

Finally, all studies show the effective use of Design Builder Software in energy analysis of all types of buildings in different climate zones and suggested to use it in early stage of design process.

2.4 Multivariate Linear Regression Approach

As mentioned earlier, the one of the thesis objectives to the develop a statistical model to predict the thermal conductivity of NAAC. Multivariate Linear Regression (MLR) analysis used to interpret the relationship between the thermal conductivity and combined mixture parameters with the physical properties of NAAC. MLR is a statistical method used to predict expected dependent variable by setting the data into a linear equation [41]. The MLR analysis will be conducted based on the following equation [42]:

$$y = b + m_1x_1 + m_2x_2 + \cdots + m_nx_n \qquad (2.3)$$

As shown in equation 2.3, y is the predicted variable, xi's are the various factors/variables, mi's are the coefficicent of varaibles and b is the constant value. As can be seen from the above equation, all independent variables are contributed for modelling of prediction equation.

Many researchers used MLR approach in order to develop a prediction model in their studies. For example, Obiyan et al. [43] predicted the compressive strength equation of bricks made from lateritic soils stabilized with bone ash using the MLR analysis. The independent variables for prediction of compressive strength were different percentage of bone ash, curing age and curing temperature. Authors developed 108 samples and used Minitab statistical software to develope the prediction model of compressive strength. Minitab statistical software analyzed the effect of each variables on compressive strength. Finally, the Minitab statistical software based on the MLR analysis provided the equation, which correlated with experimental data by 96.9%. MLR approach was also used in Sakar et al [44] studies in order to predict the Kernel weight of walnuts in Ankara. The modelling equation of kernel weight was developed successfully with 85.9% accuracy. Multivariate Linear Regression analysis was also apllied to analyze and predict the electricity consumption in the Industrial Sector of Jordan [45]. Electicity consumption as a function of electricity tariff, fuel price, produced volume, capacity and structural effects was modeled by Mintab Software. Minitab Software analyzed the significance of each variables and modeled prediction equation with the most essential variables. Finally, the accuracy of model developed in Minitab software by MLR approach was 99.3%.

In addition, Anderson et al. [46] examines the prediction of road traffic volumes in Anniston, Alabama, located in Calhoun County using the MLR approach. The major variables were roadway characteristics,such as the function classification of the road, number of lanes, population, social and economic effect. In their study, the Minitab software was apllied for all statistical analysis and the simulation developed the prediction equation with the 80% exactness. Since the Minitab provides the efficient, clear, well analyzed, easy to read and wide range of best subset options, this software is popular among researchers, as can be observed in a previous mentiod literature review.

Chapter 3. Experimental Program

3.1 Materials

As previously mentioned, normal silica-rich sand and waste soda-lime glass sand as aggregates, cement, lime, and gypsum as binders, aluminum powder as an expansion agent, water, and glass fiber were used in this study to design NAAC mixtures. Physical properties (size and gradation) and chemical properties (chemical composition and mineralogy) of each material can affect the performance of NAAC. Therefore, they were characterized before using them to produce NAAC mixtures.

3.1.1 Aggregate properties

Normal silica-rich sand and waste soda-lime glass sand were characterized based on the ASTM C-33 Standard Specification for Concrete Aggregates. According to this specification, the gradation and quality should be defined first for use in concrete. Therefore, sieve analysis was conducted to determine the size distribution of aggregates. Sieve analysis is a laboratory test that can be conducted using the required shaker apparatus and sieves with different sieve sizes. These sieves should be arranged correctly, in where the largest size sieve should be placed at the top and the smallest size sieve should be placed at the bottom followed by the pan.

After arranging all sieves correctly, approximately 0.5 kg of aggregate (normal and glass sand) was placed at the top sieve. Then, the apparatus was fixed completely and shacked for 5 minutes. After completing the shaking process, all aggregates were separated into different sieves based on their size. Finally, the mass of aggregates in each size was recorded, and the result is shown in the following Figure 3.1. Figure 3.1(a) shows the passing percentage of normal sand through sieves, whereas Figure 3.1 (b) shows the passing results of glass sand aggregates. As shown in Figure 3.1 (a), the normal sand falls out the range of upper and lower limits, specified in ASTM 33 [26]. Therefore, it can be concluded that this normal sand is finer than the sand recommended for concrete production. However, as mentioned earlier, the finer aggregates with smaller particle size should be used to get lower thermal conductivity values in materials. Therefore, this normal sand is applicable for this thesis work scope. As shown in Figure 3.1 (b), the glass sand aggregate passing at 0.3 mm and smaller sieve size falls out the limits by indicating that they are finer than the normal aggregate. The glass aggregates passing between 0.3 and 1.8 mm sieves are in the range, while others passing 2.36 and 4.75 mm sieves are out of limits indicating that this glass sand is coarser than normal

sand. Thus, it can be summarized that the amount of glass sand was estimated by taking the average from each sieve size to get uniform and constant gradation.

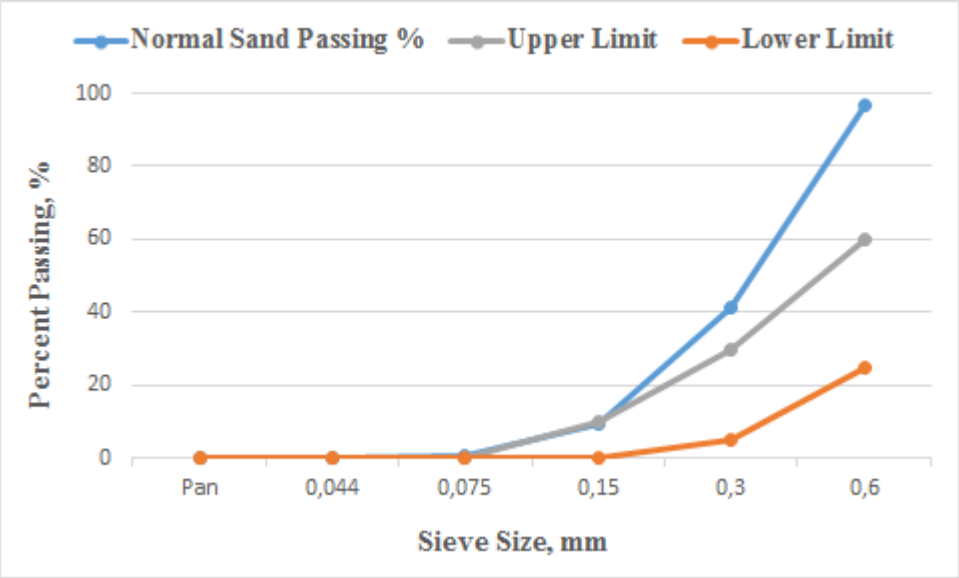

(a)

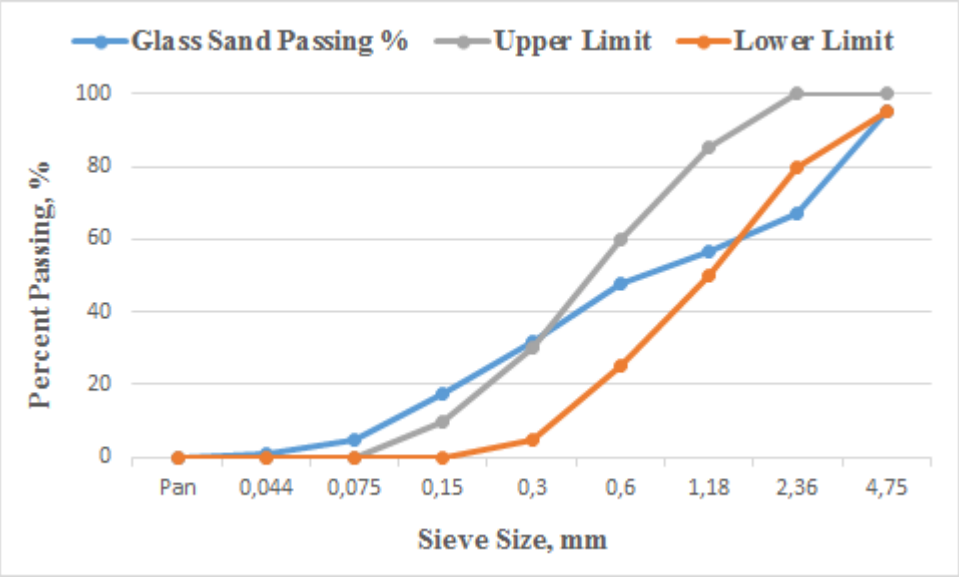

(b)

Figure 3.1. Gradation Curves of Aggregates (a) Normal Sand (b) Glass Sand

In order to identify the chemical components of ordinary sand and glass sand, X-Ray Fluorescence (XRF) was used. XRF is a non-destructive and analytical technique applicable to define the chemical composition of various types of materials such as solid, liquids,

slurries, and loose powders [27]. Tables 3.1 and 3.2 show the chemical composition results of normal sand and glass sand, respectively.

Table 3.1. Chemical Composition of Normal Sand

Components (Weight %)											
	SiO_2	CaO	Al_2O_3	Fe_2O_3	K_2O	Na_2O	MgO	TiO_2	MnO	P_2O_5	SO_3
NS	68.9	11.6	9.03	4.00	2.11	1.69	1.49	0.49	0.26	0.23	0.2

Table 3.2. Chemical Composition of Glass Sand

Components (Weight %)										
	SiO_2	CaO	O_2	Fe_2O_3	Na_2	K_2	Al_2O	P_2O_5	SrO	NiO
GS	49.6	29.5	8.809	3.2	2.8	1.46	0.88	0.64	0.63	0.375

3.1.2 Cementitious materials

Cement, lime, gypsum, and fly ash are the cementitious materials were used as cementitious materials to cast NAAC samples. The chemical composition of primary cementitious materials cement and lime was identified by using the XRF analysis, and the results are given in the following Table 3.3. As it was discussed in the literature review part, since the reaction between the alkali content in cement and silica content in glass sand can be deleterious for concrete, cement was partially replaced with fly ash in 30% content.

Table 3.3. Chemical Composition of Cementitious Materials

Components (Weight %)											
	SiO_2	CaO	Al_2O_3	Fe_2O_3	K_2O	Na_2O	MgO	TiO_2	MnO	SO_3	SG
Cement	18.2	53.8	4.01	11.79	0.79	0.16	0.58	0.2	0.46	4.32	3.14
Lime	3.92	74.3	1.501	11.94	0.07	0.122	0.237	0.1	0.50	0.18	2.20

3.2 Mix Design

As mentioned earlier in Chapter 1, the project aims to optimize the mixture proportion of NAAC containing combined glass sand and glass fiber to improve the material's thermal performance. Therefore, most literature studies were reviewed to identify mixture proportion,

which yields all mechanical, physical, and thermal properties of NAAC mixtures. Based on these studies, the following mixture design was developed for plain NAAC (Table 3.4).

Table 3.4. Properties of Plain NAAC Materials.

Material	Volume [%]	Specific Gravity	Mass [kg/m^3]
Normal sand	21,57	2,4	517,68
Cement	15,00	3,14	471,00
Lime	10,20	2,2	484,30
Gypsum	4,70	2,32	224,40
Aluminum powder	0,1	2,7	109,04
Water	48,43	1	2,70
Total	**100%**		

Then, the normal sand was replaced with glass sand and glass fiber in order to analyze their combined effect on the properties of NAAC. The material combination of the mix design of combined NAAC was generated based on literature review results and by statistical software Minitab. As shown in Table 3.5, a total of 11 different NAAC mixtures were designed.

Table 3.5 Mixture Proportion

No	**Normal Sand**	**Waste Glass Sand**	**Cement**	**Fly ash**	**Waste Glass Fiber**
M1	100	0	100	0	0
M2	85	15	100	0	0
M3	70	30	100	0	0
M4	70	30	85	15	0
M5	70	30	70	30	0
M6	70	30	100	0	1% of N. sand by volume
M7	70	30	100	0	2% of N. sand by volume
M8	70	30	100	0	3% of N. sand by volume
M9	70	30	70	30	1% of N. sand by volume
M10	70	30	70	30	2% of N. sand by volume
M11	70	30	70	30	3% of N. sand by volume

These 11 NAAC mixtures contain a partial substitution of waste soda-lime glass sand (0%, 15%, and 30%), glass fiber (1%, 2%, and 3% of normal sand by volume), and fly ash (0%, 15%, and 30%). Moreover, it should be noted that the water to cementitious material ratio of all mixtures is 0.6. Fly ash was used for preventing ASR of glass sand, and the use of fly ash can reduce the cost of NAAC in terms of sustainability. Furthermore, since the NAAC is a low-strength material, the combined use of cement and fly ash may improve the

mechanical properties, workability, and durability of NAAC. Therefore, it was decided to replace cement with fly ash (0, 15%, and 30%) and analyze its effect on the properties of NAAC.

3.3 Sample Preparation.

Before preparing and casting the samples, the total amount of samples and their volume was estimated. To increase the accuracy of test results, four samples were developed for each test. Then the average value was taken for further analysis. Moreover, each testing was made with 7-day, 14-day, and 28-day cured samples. Therefore, 12 samples for thermal conductivity, 12 samples for compressive strength, 12 samples for flexural strength, and 3 continuous samples for ultrasonic pulse velocity were prepared. The same samples were used in order to test porosity, absorption, specific gravity. Finally, 39 samples were prepared for each mixture, so 429 NAAC samples were developed for 11 mixtures.

The next step was to estimate the total volume of NAAC samples for each batch. The type of molds used for each test and their size should be estimated. The mold for thermal conductivity is rectangular with 150 mm x 150 mm x 30 mm in size. The mold for compressive strength testing is cubic with 50 mm on each side, whereas the mold for flexural strength testing is prismatic with 160 mm x 40 mm x 40mm in size. Moreover, the ultrasonic pulse velocity (UPV) samples were cast in a cubic mold and 50 mm on each side. All other information to estimate volume for each mixture is given below in Table 3.6.

Table 3.6. Volume estimation for each mixture.

Testing parameters	Mold dimensions, mm	Volume, mm3	Volume, L	Number of samples	Total volume, L
Thermal conductivity	150*150*30	675 000	0.675	12	8.1
Compressive Strength + UPV	50*50*50	125 000	0.125	12+3	1.875
Flexural Strength	160*40*40	96 000	0.256	12	3.072
Total				**39**	**13.047**

$$V_t = (150 * 150 * 30)mm3 * \frac{1L}{1000000mm3} * 12 + (50 * 50 * 50)mm3 * \frac{1L}{1000000mm3} * 15 + (160 * 40 * 40)mm3 * \frac{1L}{1000000mm3} * 12 = 13.047\ L$$

As shown in Table 3.6, the volume of each mold was multiplied by the number of samples accordingly to find the total volume of each mixture. Then, the volume proportion (Table 3.7–Column2) was multiplied by each mixture's final volume, then by specific gravity to find the mass of each material. Moreover, 10% was added to all mass because it was assumed that losses would happen during the sample preparation. The following Table 3.7 shows the adjusted mass estimation of each material for Mixture 1. The same procedure was used to estimate the adjusted mass for all mixtures.

Table 3.7. Mixture Proportion of Plain NAAC.

Material	Volume [%]	Specific Gravity	Mass [kg]	Adjusted mass [kg]
Normal sand	21,57	2,4	6.75	7.43
Cement	15,00	3,14	6.15	6.76
Lime	10,20	2,2	2.93	3.22
Gypsum	4,70	2,32	1.42	1.57
Aluminum powder	0,1	2,7	0.035	0.039
Water	48,43	1	6.32	6.95
Total	**100%**			

Then, estimated materials were mixed in the pan-type mixer with a capacity of 100-L in order to prepare and cast samples. The sample preparation consisted of the following steps, which take approximately seven minutes.

Step 1. Cement and water were placed into the mixer and mixed for 30 seconds.

Step 2. Lime, gypsum, and aluminum powder were added and mixed for another 30 seconds.

Step 3. Fine aggregates were added and mixed for 60 seconds.

Step 4. Then, mixing was stopped for 60 seconds to remove and scrap all attached materials on the pan mixer's surface.

Step 5. Finally, all materials were mixed for an additional 120 seconds.

After completion of mixing, the fresh concrete was placed into molds, which were oiled before. One of the cubic molds with dimensions of 50 mm on each side is shown below in Figure 3.2.

Figure 3.2. 50 mm Cubic Oiled Mold.

The fresh concrete was placed in two layers, and each layer was taped with a wood tamper and shake for better compaction, as shown in Figure 3.3.

Figure 3.3. Tamping procedure

After placing the samples into molds, the volume was increased, as shown in Figure 3.4 (a). It can be explained by the reaction of aluminum powder with calcium and water.

Finally, the increased volume of samples was removed from the surface of molds and covered with plastic sheets to prevent the evaporation of moisture (Figure 3.4-b).

(a) (b)

Figure 3.4 (a) Increased volume of concrete (b) After removing the increased volume.

After 48 hours, NAAC samples were demolded and cured in water baths at room temperature for 7 days, 14 days, and 28 days. After curing in a water bath for corresponding days, the samples were boiled in a 100 °C water bath for 1 day and then dried in the 85°C oven for 1 day. After that, all samples were tested, and measurements were estimated based on the corresponding testing methods and procedures described clearly in the following chapter.

3.4 Testing Methods

3.4.1 Thermal Conductivity Test

Since the thesis mainly focusing on the thermal performance of NAAC containing combined glass sand and glass fiber, the accurate estimation of thermal conductivity is essential. The special equipment “ИТС-1 «150»” is designed to measure the thermal conductivity (W/mK), thermal resistance (m2K/W), and heat flux (W/m2) of materials by the stationary heat flow method (Figure 3.5-a). As mentioned earlier, the samples for “ИТС-1 «150»” should be rectangular with 150 mm in each side, and the thickness can vary between 10 to 30 mm as shown in Figure 3.5-b.

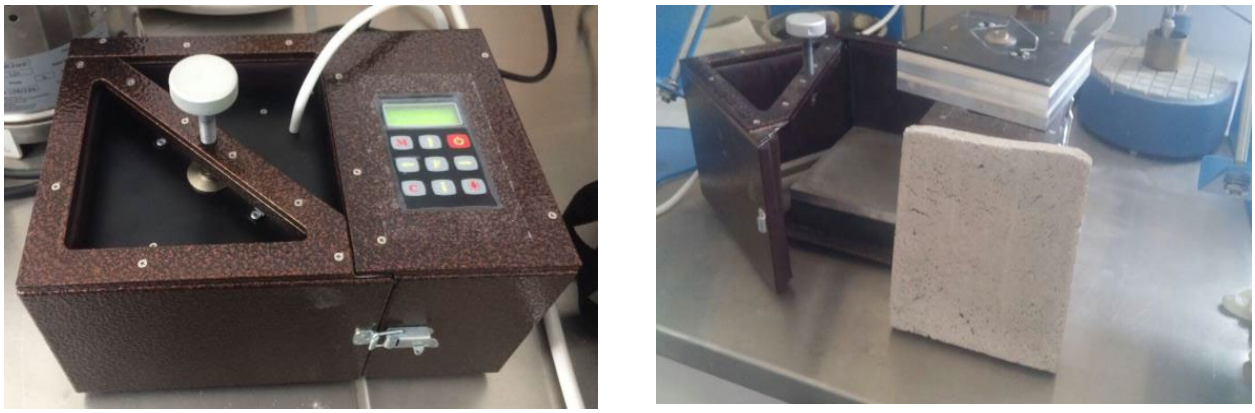

(a) (b)

Figure 3.5. (a) Thermal conductivity measure equipment

(b) 150*150*30 mm sample for thermal conductivity measurements.

The following procedures were used to estimate the thermal performance of NAAC samples:

Step 1. Equipment was checked by measuring the control sample with a known thermal conductivity value to ensure it works correctly.

Step 2. NAAC sample was inserted into the measuring cell and fixed with special settings.

Step 3. The sample was pressed with the required force with the fixing screw until three clicks appeared while turning the screw.

Step 4. One sample was measured three times, and average value of thermal conductivity was recorded for further accurate analysis.

Step 5. Each measurement took 30 minutes to 2.5 hours, and the relative error range was approximately ± 5%.

3.4.2 Compressive Strength Test.

One of the important tests that can fully characterize the material is the compressive strength test. The compressive strength of the material can be described as the capacity to resist or withstand loads before failure. During this thesis work, the compressive strength test was conducted according to ASTM C 109 specification [28]. As mentioned earlier, 50 mm cubic samples were developed for this test, and laboratory hydraulic compressive machine was used to determine its strength (Figure 3.6).

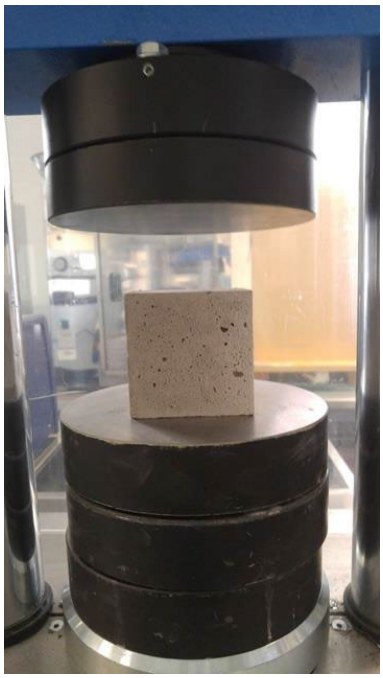

Figure 3.6. Laboratory hydraulic compressive machine

Four cubic specimens were prepared for each mixture, and the average value was taken for future analysis. The following procedures were conducted to test the compressive strength of NAAC: Firstly, the sample was placed on the center of the machine between the test surfaces. Secondly, the machine was adjusted with a loading rate of 0.6 MPa/sec. Moreover, it should be noted that the test surface of the machine could touch the sample's surface freely. After the load was applied, the maximum load at which the sample collapse occurred was recorded in the machine memory. Finally, the compressive strength was calculated by the following formula: [28]

$$\sigma_{cs} = \frac{P}{A} * \frac{1}{1000}, where$$

$$\sigma_{cs} - compressive\ strength\ in\ MPa$$

$$P - total\ maximum\ load\ in\ kN$$

$$A - loaded\ surface\ area, m2 \qquad (3.1)$$

3.4.3 Flexural Strength Test.

Another important property of the material is flexural strength, which is concrete ability to resist failure in bending. This test was conducted according to the ASTM C-348 specification, and the laboratory hydraulic compressive machine was used to conduct the test [29]. Four 40*40*160 mm prismatic samples for each batch were developed to test flexural

strength. Moreover, the three-point bent method was utilized to test the flexural strength. So, the sample should be placed so that the one load can be applied in the uppermost, and the other two can be applied in the undermost approximately 53 mm apart from each other. All other procedures are the same with the compressive strength testing. Finally, the following equation used to calculate the flexural strength [29]:

$$\sigma_{fs} = \frac{1.5 * F_{max} * L}{bd^2} * \frac{1}{1000}, where$$

$$\sigma_{fs} - flexural\ strength\ in\ MPa$$

$$F_{max} - maximum\ load\ in\ kN$$

$$L - length\ of\ specimen, m$$

$$b - width, m$$

$$d - depth, m \quad (3.2)$$

3.4.4 Ultrasonic Pulse Velocity Test.

The following important test that was conducted in this thesis work is Ultrasonic Pulse Velocity Test (UPV). The UPV is a non-destructive test, which can characterize the homogeneity, porosity, quality, defects, and cavities in the concrete. The UPV test was conducted according to ASTM C597 Specification, and the ultrasonic pulse tester machine was used to perform this test [30]. There was a pulse generator, amplifier, time measuring circuit, time display unit, connecting cables, transmitting transducer, and transducer in the apparatus. The transducers' surface was covered with special liquid, and then they were stuck to concrete sides, as shown in Figure 3.7.

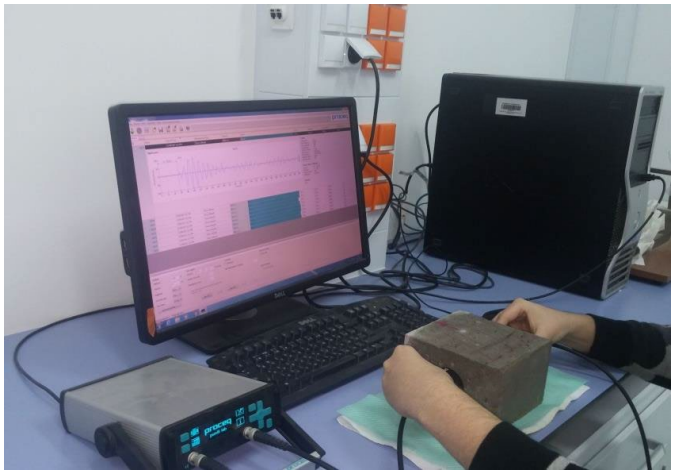

Figure 3.7. Measurement of UPV of NAAC.

When the pulse generator produced pulses, these pulses are passed through the concrete by the transmitting and receiving transducers. Moreover, this tester machine was connected to the computer. All results are monitored on the computer and recorded for further analysis. Two types of samples were used to estimate the pulse velocity. The first one is the non-continuous cured samples, which means that they were tested and broken. Another type is continuous cured samples, in which samples were tested for pulse velocity and cured again in water for the next corresponding days, then tested again for pulse velocity. The results of two different ways of estimation of pulse velocity were described fully in the test results and discussion part.

3.4.5 Porosity, Density, and Absorption.

The physical properties of concrete were also analyzed in this thesis work. Since all thermal characteristics, mechanical and physical properties are related to each other, it is essential to find their relations. In order to estimate porosity, density, and absorption, the mass of samples after each step should be recorded. As it was mentioned earlier, after 48 hours, the samples were demolded, and their mass was measured (M_0). Then, the samples were cured in water baths at room temperature for 7 days, 14 days, and 28 days and after corresponding days, their mass was measured (M_1). After the samples were boiled in a 100°C water bath for 1 day (M_2) and were immersed in water (M_3). Finally, the samples were dried in the 85°C oven for 1 day (M_4). Accordingly, the following equations were used to estimate physical characteristics:

$$Porosity = \frac{Saturated\ after\ boiling\ weight - Oven\ dry\ weight}{Saturated\ after\ boiling\ weight - Immersed\ in\ water\ weight} * 100\%$$

$$= \frac{M_2 - M_4}{M_2 - M_3} * 100\%$$

$$Density = \frac{Oven\ dry\ weight}{Saturated\ after\ boiling\ weight - Immersed\ in\ water\ weight} * 100\%$$

$$= \frac{M_4}{M_2 - M_3} * 100\%$$

$$Absorption = \frac{Saturated\ after\ boiling\ weight - Oven\ dry\ weight}{Oven\ dry\ weight} * 100\%$$

$$= \frac{M_2 - M_4}{M_4} * 100\%$$

Chapter 4. Test Results and Discussion

This chapter consists of three main section and each part includes the analysis of experimental test results. The section 4.1 explains the relationship between the physical and mechanical properties of NAAC, in which the density, porosity, absorption, compressive and flexural strength will be describe fully in each subsections. The section 4.2 interprets the relationship between the mixture parameters and thermal conductivity of NAAC. Here the effect of glass sand, glass fiber, fly ash and their combined effect on the thermal property of NAAC will be characterized. The section 4.3 describes how physical properties affect on the thermal property of NAAC. All eleven mixtures were divided **by Series** for easier deep analysis. **The Series 1** includes the first three mixtures (M1, M2 and M3) in which the normal sand was partially substituted by glass sand (0, 15% and 30%). The Series 2 includes the Mixture 3, Mixture 4 and Mixture 5, where the cement was partially replaced with fly ash. The Series 3 includes the Mixture 6, 7 and 8, which contains 1%, 2% and 3% replacement of glass fiber by volume of normal sand. The Series 4 contains the last three mixtures, which contains the combined glass sand, glass fiber ad fly ash. So, the overall results and by series results are analyzed below in following chapters.

4.1 Physical and Mechanical Properties of NAAC

4.1.1. Relationship between dry density and porosity

This section investigates the relationship between the density and porosity of NAAC. According to the test results, it can be observed that as the porosity increases, the density of NAAC decreases. Since, the porosity is interpreted as the voids generation and volume increase, which makes the material lighter, the density of concrete becomes lower. Therefore, the porosity and density are in inverse relation. This observation matches with the result of previous studied papers. Based on the curing age effect, the density of 14-day cured samples is lower than the density of 7-day cured samples. However, the density of 28-day cured samples is higher than the 7-day and 14-day cured sample results (Appendix A). The increase of curing age has a long – term effect on the hardening of NAAC, because of the hydration of cementitious materials. The hydration process is result of the chemical reaction between the water and cementitious materials. As the hydration process occurred, the voids becomes less. Therefore, the density is higher in 28-day cured samples.

The following Table 4.1 shows the relationship between the porosity and density of all 7-day, 14-day and 28 – day cured samples by R^2 value. R^2 value indicates the exactness of

fitting between properties. The high R^2 value indicates the good exactness, whereas the lower R^2 value indicates the poor exactness of relations between properties. As can be seen in Table 4.1, the relationship between the porosity and density is high in 14-day cured samples. By series analysis show that the Series 3 consists of the glass fiber has a highest density and the lowest porosity among other series (Appendix A). Moreover, as it shown in Table 4.1 and Figure 4.1, all Series have a high R^2 between porosity and density except the Series 2 in 7-day and 28-day cured sample results. Since the Series 2 samples consist partial replacement with fly ash (15% and 30%), the porosity of these samples becomes higher, but the density was not changed very much. Therefore, the relationship of density and porosity is lower in Series 2 than other samples. Since, the density is lower in 14-day cured samples and its relationship with porosity (R^2) is higher, the 14-day cured samples were taken for further analysis of NAAC properties. The density and porosity results are shown in Appendix A.

Table 4.1 Relationship between porosity and density

	7 day	14 day	28 day
	R^2		
Overall	46,24%	63,36	10,09
Series 1	70,73	95,74	99,99
Series 2	0,9	99,63	17,1
Series 3	81,99	98,26	84,19
Series 4	98,82	81,14	99,88

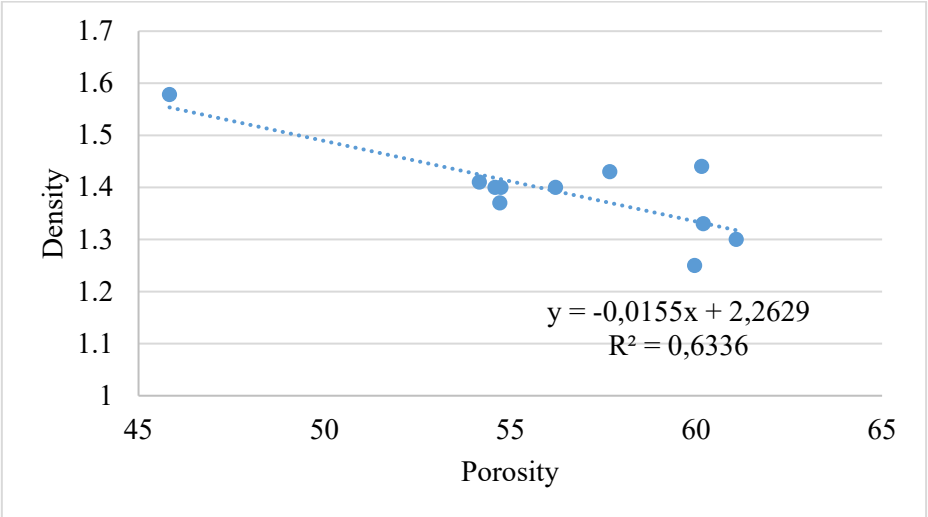

(a)

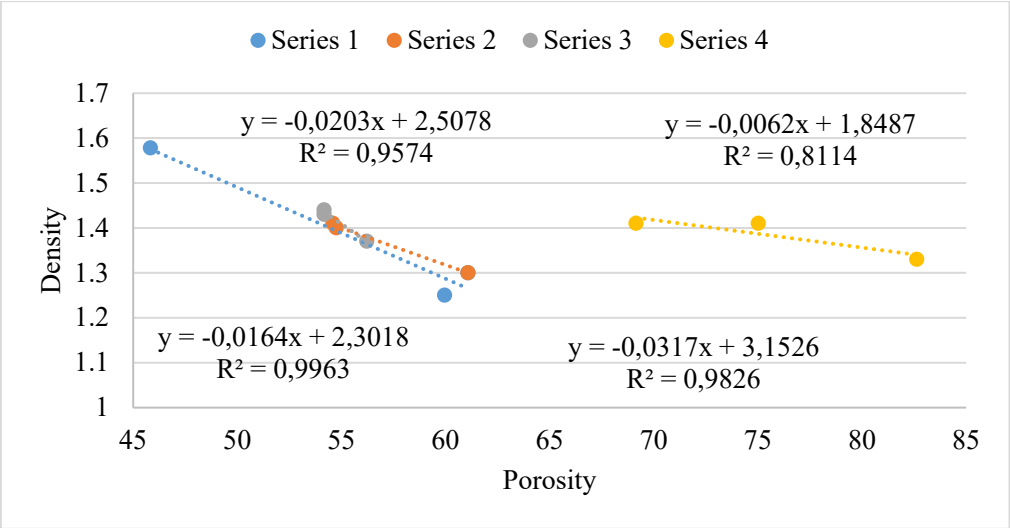

(b)

Figure 4.1. The relationship between density and porosity (a) overall data (b) by series

4.1.2. Relationship between dry density and water absorption

This section describes the relationship between the density and water absorption of NAAC. Based on the test results, it was observed that the samples with lower density absorbs more water than those with higher density. Thus, the increase of density leads to the decreasing of absorption capacity of materials. As a porosity, the absorption and density are reciprocal properties with each other. As can be seen in Table 4.2, the fitting exactness R^2 again is higher in 14-day cured samples by overall. Generally, the R^2 is high in all cured samples, except Series 2 in 7-day and 28-day cured samples. These Series 2 sample results lead to minimize the overall R^2 of 7-day and 28-day cured sample properties. As it was mentioned earlier, the samples of Series 2 partially consist the fly ash content (15% and 30%) instead of cement. So, the result of samples with fly ash significantly affects to the reducing of R2 value in 7-day and 28-day cured results. Therefore, since the 14-day cured samples demonstrates high and exact relationship in overall and by series analysis, these samples were decided to taken for further analysis of NAAC properties.

Table 4.2. Relationship between density and absorption

	7 day	14 day	28 day
Overall	58,07%	69,52	32,89
Series 1	80,5	99,88	90,09
Series 2	27,61	99,68	28,2

Series 3	86,44	99,89	91,2
Series 4	99,97	81,14	100

The following Figure 4.2 shows the density and absorption results of 14-day cured samples by overall and by series. Overall analysis (Figure 4.2 – a) demonstrates that the density increase leads to the reducing of absorption capacity in NAAC samples. Based on the by series analysis, the highest R^2 was observed in Series 3 samples, because these samples have the highest average density and the lowest average absorption capacity among other samples. The lowest R^2 was observed in Series 4 samples, which has the maximum average absorption capacity. Moreover, based on the test results, it was observed that in Series 1 and 2 samples, the absorption decreases and density increases by the curing age increases. It can be explained by the hydration process between the water and cementitious materials, in which material becomes harder. Therefore, as the curing age increased, the density also increased, but the absorption decreased. However, in Series 3 and 4 samples, as curing age increases the absorption also growth, and it might be explained because of the effect of glass fiber content. The density and absorption results are shown in Appendix A.

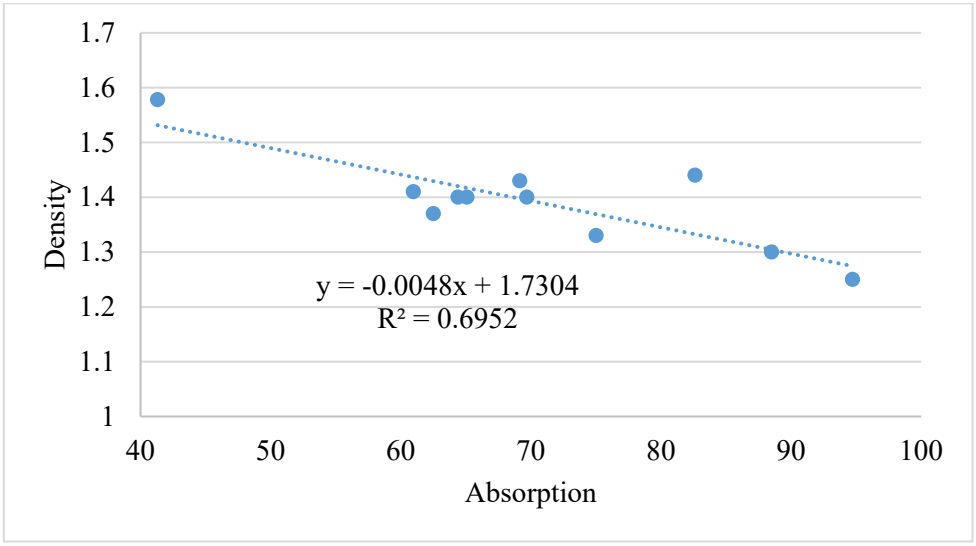

(a)

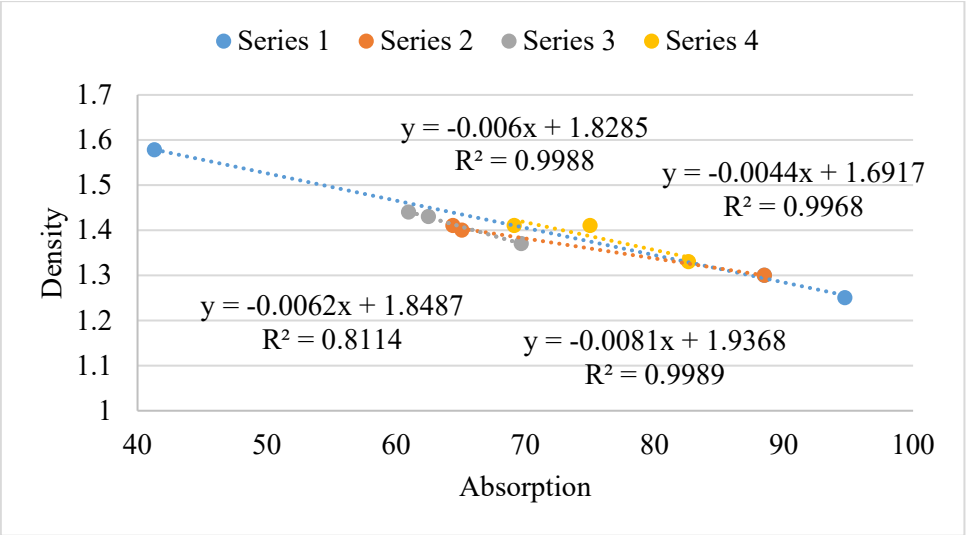

(b)

Figure 4.2. The relationship between density and absorption (a) overall data (b) by series

4.1.3. Relationship between porosity and water absorption

This part analysis the relationship between the porosity and absorption of NAAC samples. According to the test results, the increase of absorption capacity leads to increase in porosity of NAAC samples. Thus, porosity and water absorption is in direct relationship. Because, as the concrete absorbs water, its volume will be expanded, which leads to the porosity increases. As can be seen in Table 4.3, the porosity and absorption is fitting very well, since R^2 is high in all cured sample results, except Series 2 in 28-day cured samples. Again, the fly ash significantly affects to the fitting coefficients between porosity and absorption, as the earlier result of other properties correlation and they were explained above. The maximum porosity and absorption in average were observed in 7-day cured series 2 samples, which consist fly ash (see Appendix A). Therefore, it can be concluded that in short term effect, the fly ash affects positively, but in terms of long-term effect the fly ash replacement affects negatively to the correlation of properties. Moreover, the Since, the correlation between all properties, as density, porosity and absorption is very high in 14-day cured samples; these samples are decided to choose for further analysis of energy saving effect, in modelling of prediction equation, and in feasibility analysis.

Table 4.3 Relationship between porosity and absorption

	7 day	14 day	28 day
Overall	96,17%	86,34	18,45

Series 1	98,7	97,04	88,08
Series 2	63,57	100	30,46
Series 3	99,63	97,26	98,84
Series 4	99,19	100	99,92

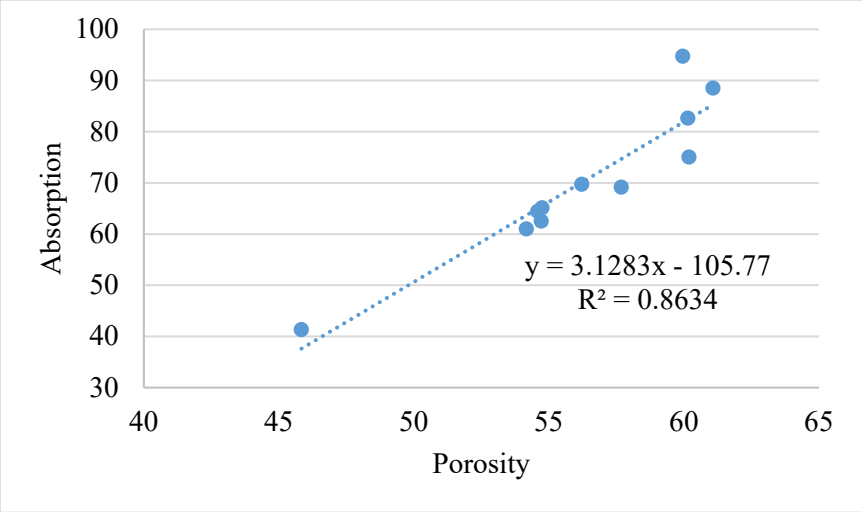

(a)

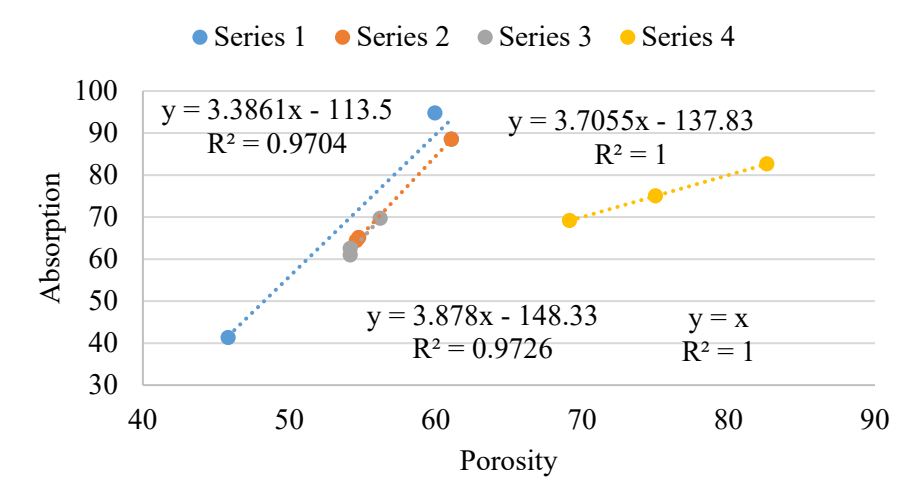

(b)

Figure 4.3. The relationship between porosity and absorption (a) overall data (b) by series

4.1.4. Compressive strength development

The following Figure 4.4 – Figure 4.7 demonstrates the effect of mixture parameters on the compressive strength of NAAC. It should be noted that the average of four samples is given in the graph. As can be observed from Figure 4.4, the replacement of normal sand with glass sand increases the compressive strength of NAAC. Moreover, the increase of glass sand

content from 15% to 30% leads to the compressive strength enhancing. For example, in 14-day cured samples, the compressive strength of Mixture 2 containing 15% glass sand is 0.843 MPa, whereas the compressive strength of Mixture 3 containing 30% glass sand is 1.083 MPa, thus it was increased by 28.46%. Moreover, the compressive strength of mixture 3 containing 30% glass sand is three times higher than the batch mixture (M1). Therefore, it can be concluded that the partial substitution of normal sand with waste soda-lime glass sand affects absolutely positively to the compressive strength of all NAAC samples.

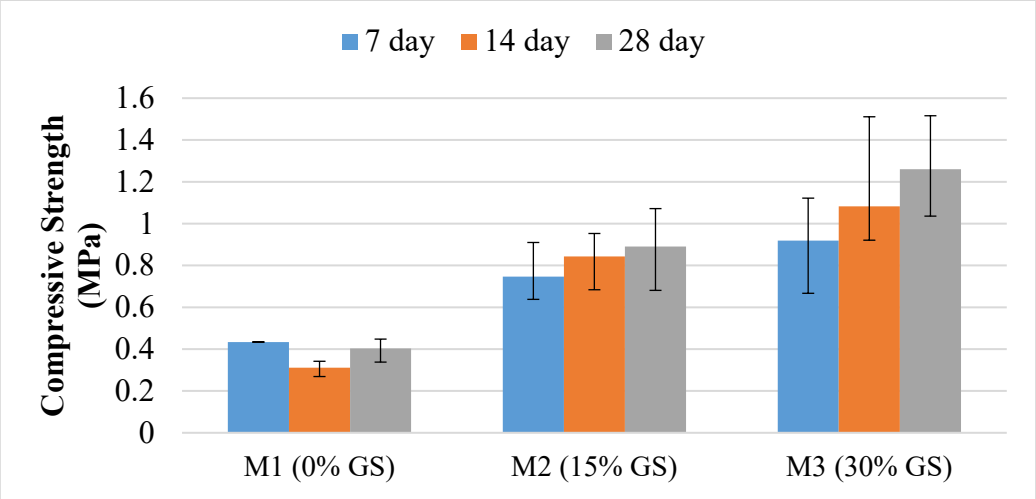

Figure 4.4. The compressive strength of NAAC containing glass sand

The following Figure 4.5 indicates the compressive strength of NAAC containing 30% glass sand and partially substituted fly ash (15% and 30%). As can be seen from results, the 15% replacement with fly ash affects positively to compressive strength of NAAC, because it was increased from 0.919 MPa to 1.29 MPa, from 1.083 MPa to 1.695 MPa, and 1.26 MPa to 1.77 MPa in 7-day, 14-day and 28-day cured samples, respectively. However, the 30% substitution with fly ash negatively affects to the compressive strength of NAAC. As can be observed in Mixture 5 (30% fly ash), the compressive strength was dropped down to 1.6 and 1.8 times in 7-day and 14-day cured samples, respectively than the Mixture 4 (15% fly ash). However, in Mixture 5, the dropping of compressive strength was insignificant in 28-day cured samples. It can be explained by the hydration process between water and cementitious materials in mixtures. Moreover, the physical characteristics of samples can also affect to the strength development of material. For example, the 7-day density to porosity ratio (D/P) in mixture 4 was 0.027 while in mixture 5 it was 0.023. Since the density to porosity ratio was decreased in Mixture 5, the strength was also dropped from 1.295 MPa to 0.798 MPa at this mixture. Finally, it can be summarized that the replacement of cement with 15% fly ash

enhances the compressive strength, but the 30% replacement with fly ash reduces the compressive strength of NAAC.

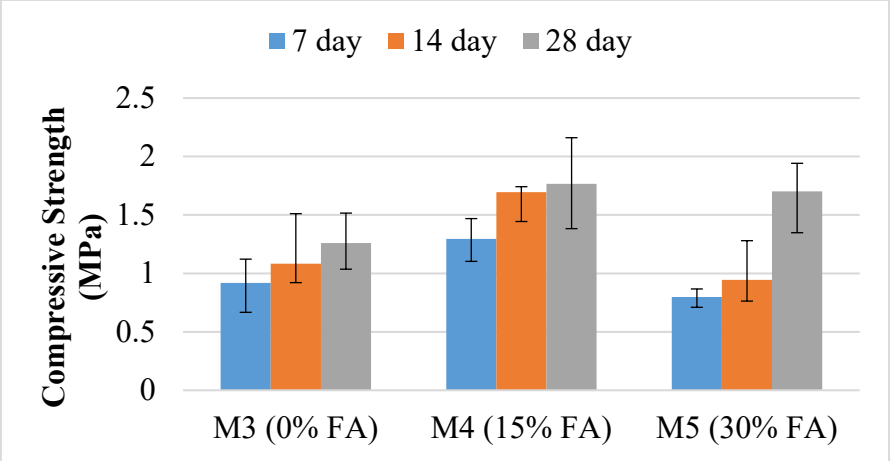

Figure 4.5. The compressive strength of NAAC containing fly ash

The following Figure 4.6 shows the effect of glass fiber on compressive strength of NAAC. As can be clearly seen from figure, as the glass fiber content increases, the compressive strength also increases. For example, the average compressive strength of 14-day cured mixture 8 samples containing 3% glass fiber is 2 times higher than that samples containing 1% glass fiber. Moreover, the maximum compressive strength was observed in 28-day cured samples, which contain 3% glass fiber. It can be explained by the hardening of concrete because of hydration process and with the maximum amount of glass fiber. The compressive strength of these samples (28-day cured Mixture 8) is 5 times higher than the compressive strength of the batch specimen. Finally, it can be concluded that the synergistic effect of waste soda lime glass sand with glass fiber on compressive strength development of NAAC samples are clearly shown.

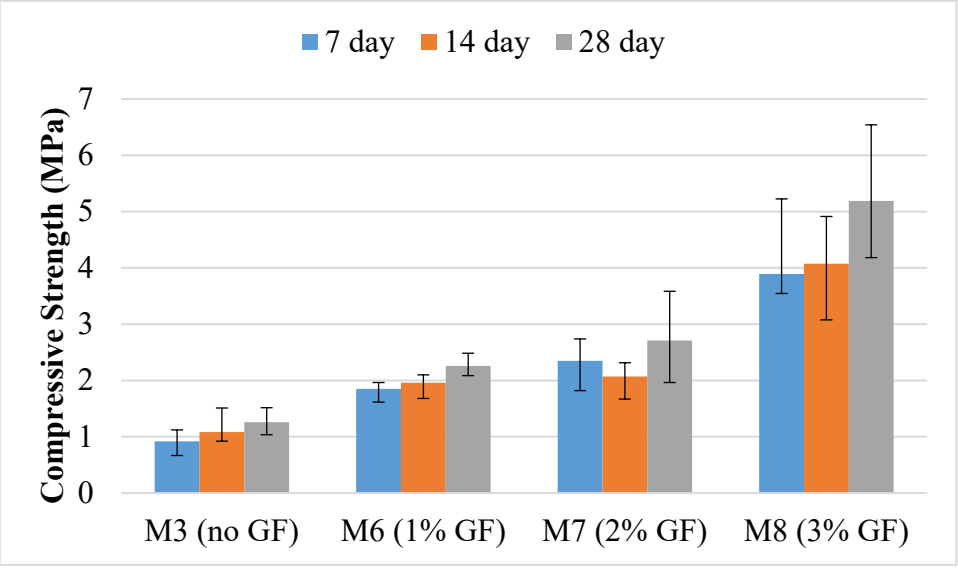

Figure 4.6. The compressive strength of NAAC containing glass fiber

The development of compressive strength of Series 4 mixtures, containing combined glass sand, glass fiber and fly ash is fluctuated, as can be observed in the following Figure 4.7. For example, the compressive strength of 7-day cured samples are increased with increase of glass fiber, whereas the 14-day compressive strength are decreased. These inconsistent strength developments are probably due to the physical properties of these samples, which are the result of process of casting samples. Only, the 28-day cured compressive strength is constantly increased and it might be explained with the hydration process.

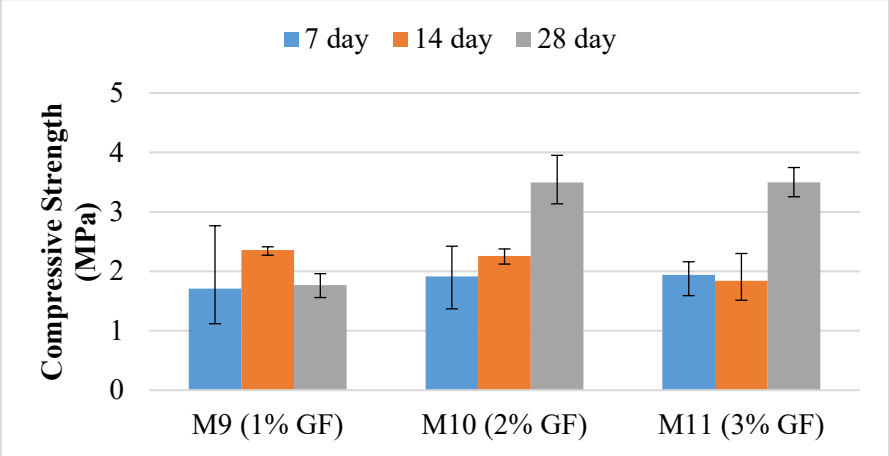

Figure 4.7. The compressive strength of NAAC containing combined glass sand, glass fiber and fly ash

4.1.5. Flexural strength development

The following Figures 4.8 – 4.11 are investigated the effect of mixture parameters on the flexural strength of NAAC samples. The Figure 4.8 explains the effect of glass sand on the flexural strength of NAAC. According to the results, the increase of glass sand positively affects to the increase of flexural strength of NAAC in overall. As can be seen from figure, the flexural strength of samples containing the 15% glass sand is higher than the flexural strength od samples containing 30% glass sand. However, the difference is not very much. For example, the 7-day flexural strength of mixture M2 was 1.86 MPa, whereas the flexural strength of 7-day cured Mixture 3 samples was 1.78 MPa. Only the 14-day cured samples containing 15% glass sand is assessed as an exception, because its flexural strength was dropped. It can be explained by their physical properties; because the Mixture 2 has characteristics of the lowest density, the highest porosity and the highest absorption than other samples (see Appendix B). These material characteristics obviously explain why the flexural strength of 14-day cures Mixture 2 samples is the lowest one.

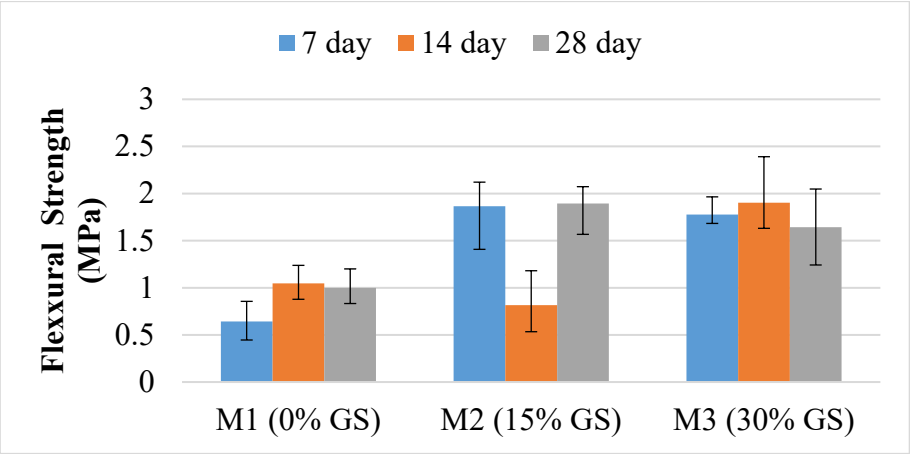

Figure 4.8. The flexural strength of NAAC containing glass sand

The following Figure 4.9 describes the effect of fly ash content on the flexural strength of NAAC. According to the results, the 15% replacement with fly ash negatively affects to the flexural strength of NAAC. Because the flexural strength was dropped from 1.778 MPa to 1.444 MPa in 7-day cured samples, from 1.903 MPa to 1.394 MPa in 14-day cured samples, and from 1.643 MPa to 1.611 MPa in 28-day cured samples. However, the Mixture 5 containing 30% fly ash has a higher flexural strength than the Mixture 3 and 4, except the 28-day cured Mixture 5. Again, the inconsistent development of flexural strength is probably due to the physical characteristics of these mixtures, which is shown in Appendix B.

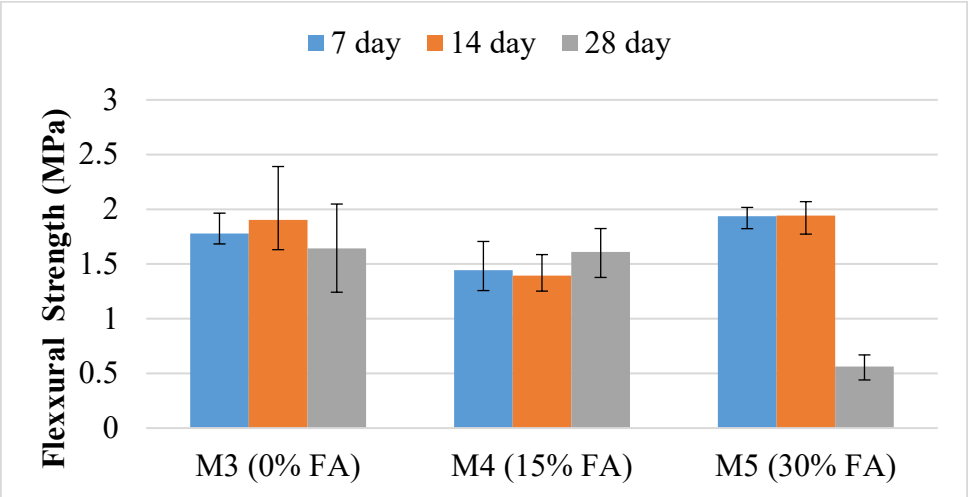

Figure 4.9. The flexural strength of NAAC containing fly ash

The following Figure 4.10 interprets the effect of glass fiber on the improvement of flexural strength of NAAC. Based on the experimental results, when the glass fiber replacement was used together with 30% glass sand, the flexural strength was increased. The 1% and 2% addition of glass fiber insignificantly affects to the flexural strength development, while the 3% glass fiber leads to the considerable increase in flexural strength.

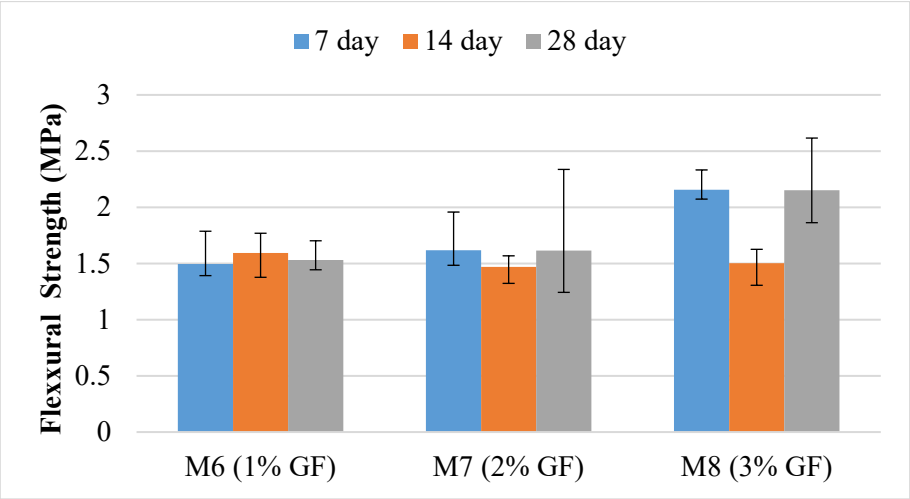

Figure 4.10. The flexural strength of NAAC containing glass fiber.

The addition of fly ash to the combined glass sand and glass fiber mixture had an unstable effect on flexural strength development of NAAC. For example, the 30% fly ash and 30% glass sand with the increase of glass fiber from 1% to 3% has a great effect on the 7-day cured flexural strength enhancing. However, for other 14-day and 28-day cured it affects insignificantly. These inconsistent results are also can be explained by the physical properties of mixtures, which are shown in Appendix B.

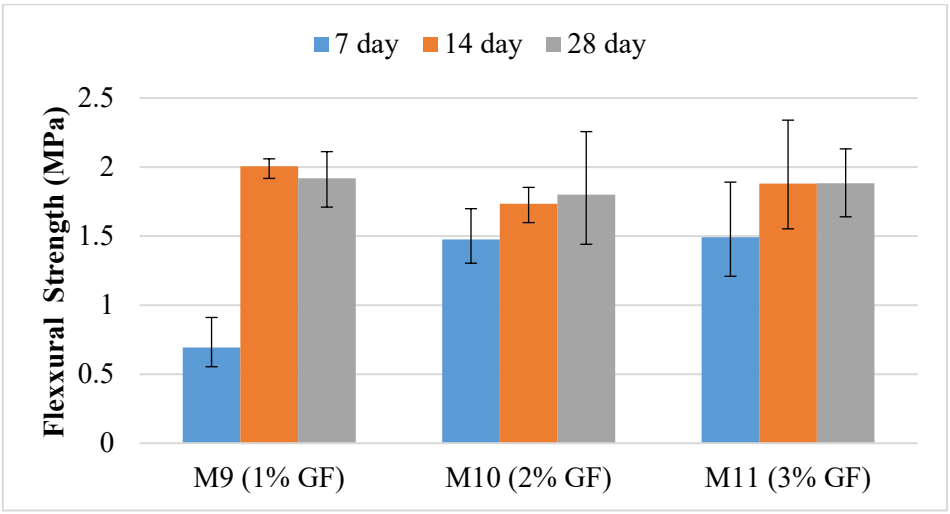

Figure 4.11. The flexural strength of NAAC containing combined glass sand, glass fiber and fly ash

4.1.6. Relationship between ultrasonic pulse velocity and compressive strength

This section analyses the relation between the compressive strength and ultrasonic pulse velocity (UPV). It should be noted that the UPV was tested firstly on sample, and then the compressive strength of that sample was measured. Therefore, the goal of this section is to investigate their effect on each other. According to the results, the material with higher

velocity also has a higher compressive strength. Because, UPV testing is used in order to determine the quality, continuity and integrity of concrete structure, so the higher velocity indicates a good quality with higher strength, whereas a lower velocity indicates the structure with cracks and voids. In this thesis work, the experimental test results also match with the theoretical background. As an example, the 7-day cured sample results are shown in the Figure 4.12, in which the direct proportion of UPV and compressive strength can be clearly observed. Moreover, it should be noted that the correlation coefficients of all 7-day, 14-day and 28-day cured samples are high as 87.83%, 87.06%, 90.26%, respectively (Table 4.4). Moreover, by series analysis also demonstrate the excellent relationship between the UPV and compressive strength of NAAC, as can be seen from Figure 4.12-b

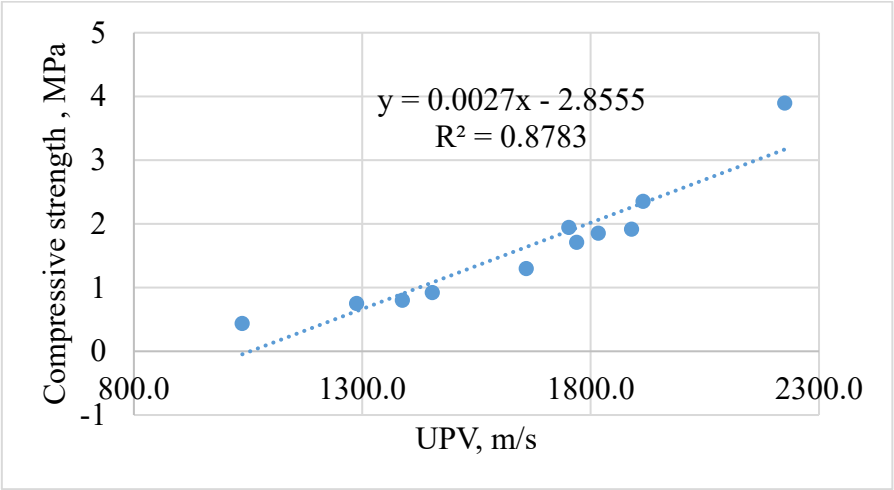

(a)

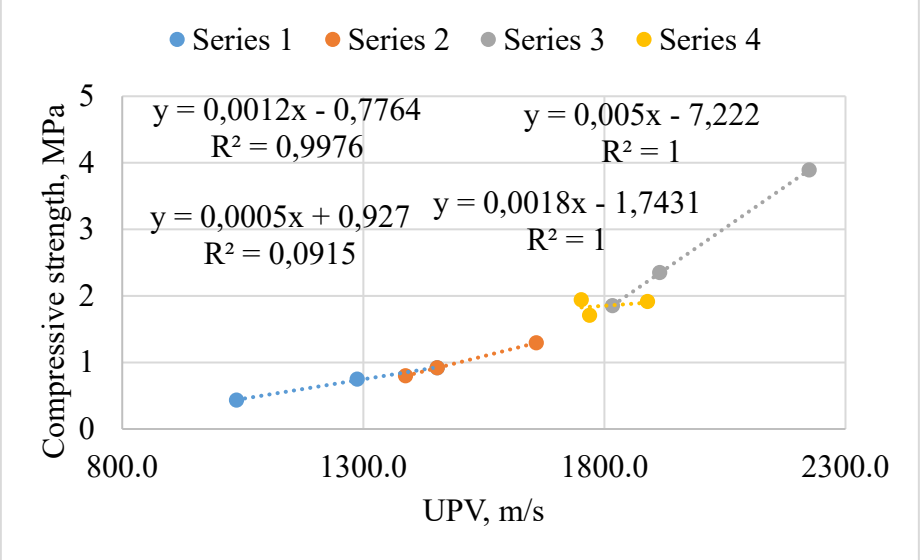

(b)

Figure 4.12. The relation between the UPV and compressive strength.

Table 4.4 Relationship between the compressive strength and UPV

	7-day	14-day	28-day
Overall	87,83	87,06	90,26
Series 1	99,76	99,71	95,88
Series 2	100	95,95	61,08
Series 3	100	52,62	100
Series 4	91,5	91,74	98,8

4.2 Relation between mixture parameters of NAAC and thermal conductivity

4.2.1. Effect of glass content on thermal conductivity

This section analyses the effect of waste soda lime glass sand on the thermal properties of NAAC and Figure 4.13 shows its result. The average value of four samples is indicated in the graph. According to the test results, as the glass aggregate content increases, the thermal conductivity decreases. For example, in a 7-day cured samples, the thermal conductivity of sample containing only normal sand (M1) was 0.225 W/K, then the replacement of normal sand with 15% and 30% glass sand leads to decrease the thermal conductivity down to 0.1325W/K and 0.1308W/K, respectively. It means 7-day cured thermal conductivities reduced by 41.1% and 41.9% by substituting normal sand with 15% and 30% glass sand, respectively. Moreover, the 14-day cured samples demonstrated the same results by decreasing the thermal conductivity from 0.2104 W/K to 0.1251 W/K when the 30% glass sand was added. In addition, in the results of 28-day cured samples the same trend can be demonstrated, because it was dropped to 39.8 % and 38% than plain concrete by replacing normal sand with 15% and 30% glass sand, respectively. As can be observed from test results, in 7-day cured samples, samples containing 30% glass sand shows better thermal insulation than 15% replacement, whereas in 14-day and 28-day cured samples, samples containing 15% glass sand demonstrates better thermal property than samples containing 30% glass sand. Therefore, besides the mixture parameters, the effect of porosity, density and absorption on thermal conductivity will be analyzed further in order to make a precise conclusion.

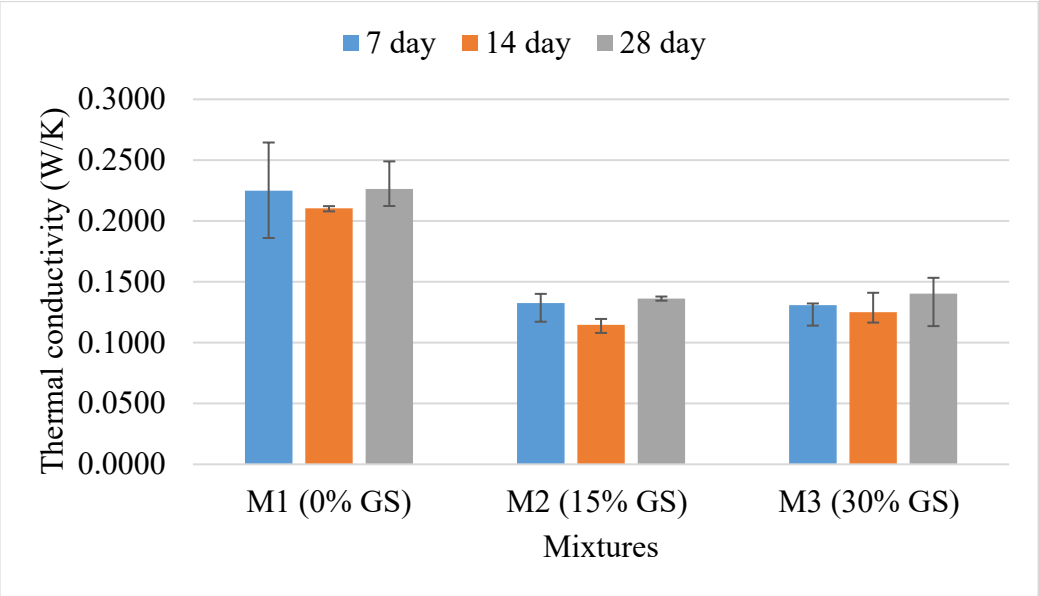

Figure 4.13. Thermal conductivity of NAAC containing glass sand

4.2.2. Effect of fly ash content on thermal conductivity

This chapter describes the effect of fly ash on thermal property of NAAC. As it was mentioned earlier, Series 2 contains three different mixtures, which are includes the partial substitution of cement with fly ash (0%, 15%, and 30%). It should be mentioned that fly ash was added to that mixture, which includes 30% of glass aggregate in order to analyze the combination of glass sand with fly ash on properties of NAAC. As can be seen from Figure 4.14, the substitution of cement with fly ash leads to increase of thermal conductivity of NAAC. This trend is clearly shown in a 14-day and 28-day cured samples. For example, in 14-day cured samples, the addition of 15% fly ash (M4) increases the thermal conductivity by 27%, and 30% substitution of fly ash (M5) leads to increase the thermal conductivity up to 41% than samples which contains 0% fly ash (M3). Moreover, in 28-day cured samples, 15% replacement of cement with fly ash increased the thermal conductivity of NAAC from 0.1403 W/K to 0.2167 W/K, which is 54.5% increasement, whereas 30% replacement with fly ash grows it up to additional 3.23 %. Only in 7-day cured samples, the 15% and 30% substitution of cement with fly ash has an insignificant effect on thermal property of NAAC, which contains only 5% and 1.15% growth on thermal conductivity respectively. It again proves that the effect of fly ash is insignificantly in short-term periods and its effect is greater in long-term periods. In addition, it can be explained because of the less hydration process in a 7-day cured.

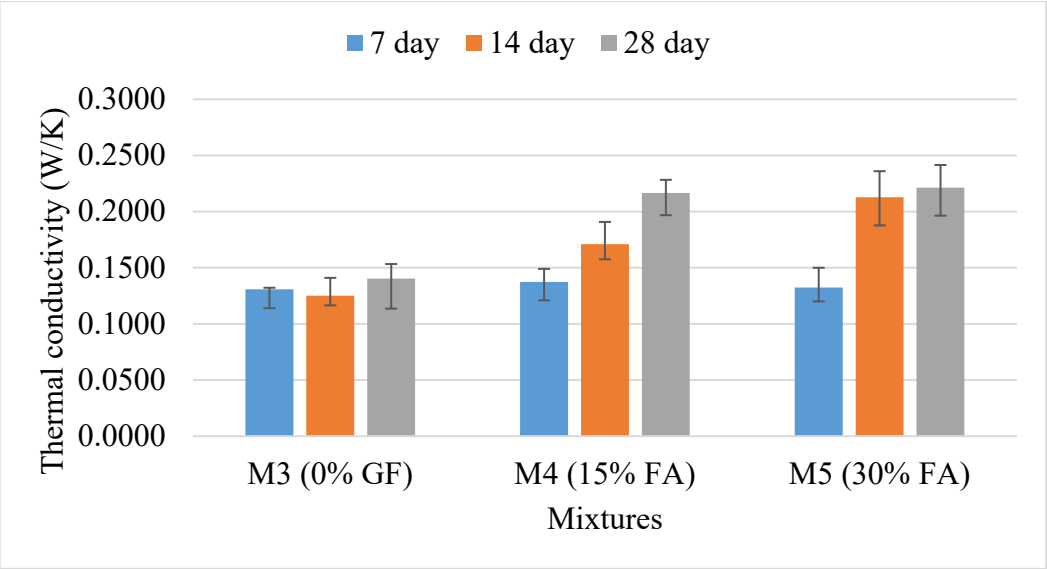

Figure 4.14. Thermal conductivity of NAAC containing fly ash

4.2.3. Effect of fiber content on thermal conductivity

This chapter explains the combined effect of glass sand and glass fiber on thermal property of NAAC. The following three mixture parameters (M6, M7 and M9) include the constant 30% substitution with glass sand and 1%, 2% and 3% glass fiber. As it was expected, mainly increase in glass fiber content results in increasing the thermal conductivity of NAAC, except 28-day cured samples. In 7-day cured samples, the thermal conductivity of sample contains 0% glass fiber (M3) is 0.1308W/K. Then, 1%, 2% and 3% substitution the volume of normal sand with glass fiber increased it up to 0.1596W/K, 0.1861W/K and 0.1670 W/K respectively. In general, 1%, 2% and 3% replacement with glass fiber leads to 22%, 42.3% and 27.7% growth of thermal conductivity, respectively. In a 14-day cured samples, the same results were observed, in which the thermal conductivity growth is 44%, 49.7% and 57.3% when 1%, 2% and 3% glass fiber was added. As can be seen from the following Figure 4.15, in 28-day cured samples some exceptions exist. Because 1% replacement of glass fiber increases thermal conductivity from 0.1403W/K to 0.2202 W/K, which is 57% growth. However, 2% glass fiber decreases the thermal conductivity to 0.1436 W/K, which is 34.8% drop. Finally, 3% replacement with glass fiber increases it up to 0.2 W/K. As it was observed, there is no clear development in a thermal conductivity of 28-day cured samples. This inconsistent result can be explained by the physical properties of NAAC. For example, in 28-day cured samples, the P/D of M6 is 40.3, the P/D of M7 is 43.1 and the P/D of M8 is 37.4. These physical characteristics are obviously affected to the inconsistent development of thermal properties of NAAC.

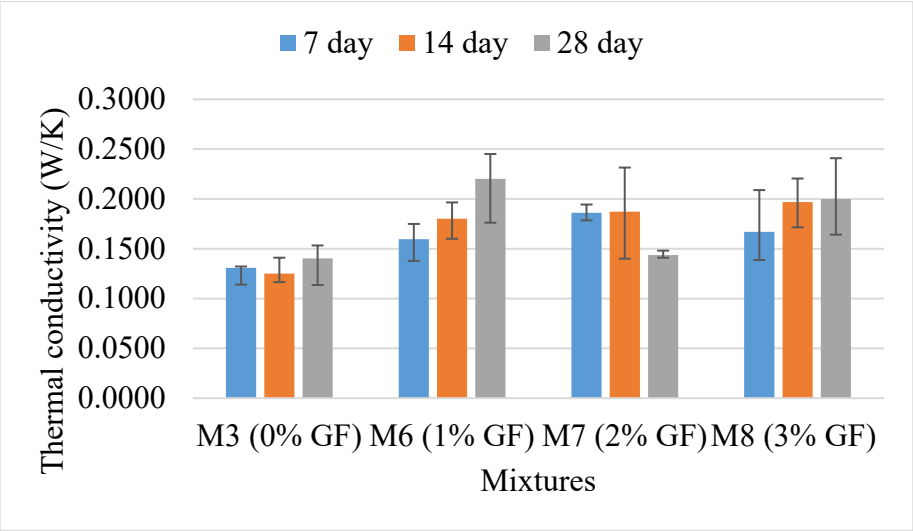

Figure 4.15. Thermal conductivity of NAAC containing glass fiber

The final three mixtures (M9, M10 and M11) were developed by combining 30% glass sand, 30% fly ash, 1%, 2% and 3% glass fiber respectively and the thermal conductivity results of these mixtures are shown in the Figure 4.16. The combination of glass fiber with fly ash negatively affect to the thermal property of NAAC, because it increases the thermal conductivity of NAAC.

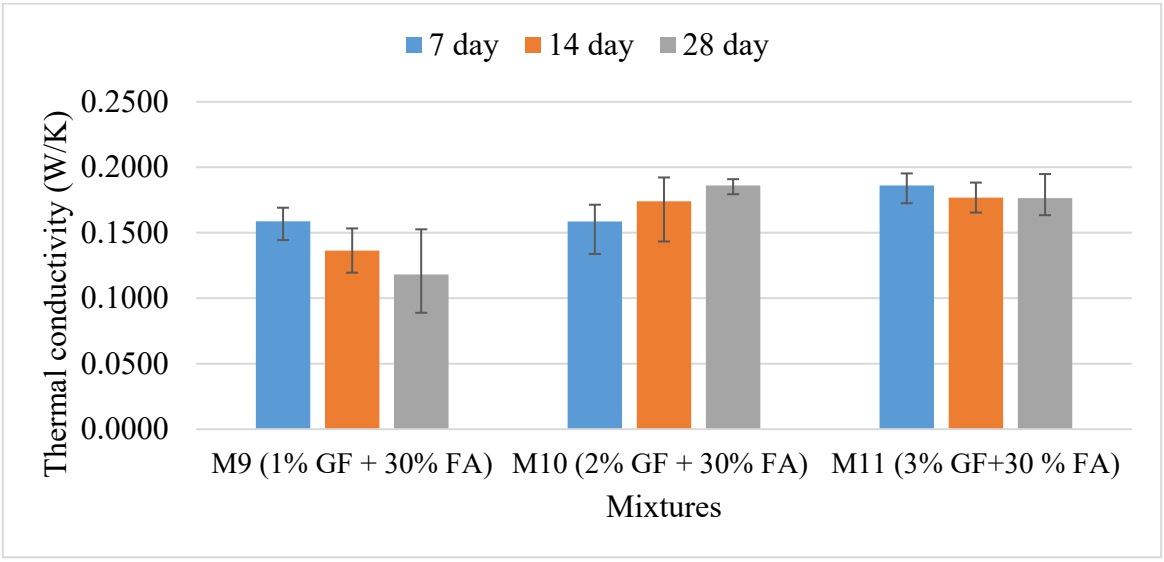

Figure 4.16. Thermal conductivity of NAAC containing glass fiber with fly ash

4.3 Relation between physical properties of NAAC and thermal conductivity

4.3.1. Effect of curing age on thermal conductivity

The following Figure 4.17 demonstrates the effect of curing age on thermal conductivity of NAAC. The thermal conductivity was measured at 7-day, 14-day and 28-day curing ages. Their relationship was analyzed by series. As can be seen in Figure 4.17-a, the thermal conductivity of Series 1 samples are inconsistent, since the λ of 14-day cured samples is decreased, while in 28-day cured Series 1 samples λ increases. In addition, also in Series 2 and Series 3 samples, the thermal conductivity is mainly increases as the curing age increases. The direct relationship of curing age with thermal conductivity (increased curing age → higher thermal conductivity) corresponds to previous gained studies. Generally, the λ of NAAC mainly depends on the λ of composite materials and the void spaces between the particles. According to the studies, the curing age affects on the hydration of cementitious materials. As the hydration process occurred, the voids spacing between the composite particles become less, which leads to the decreasing of porosity. Therefore, the thermal conductivity becomes higher as the curing age increases as it can be observed in samples of Series 1, 2 and 3, in spite of some exceptions, as the Mixture 7, 9 and 11. In order to identify the reason of declining the thermal conductivity of this samples, the further analysis between the physical properties, thickness and thermal property of NAAC should be proceeded.

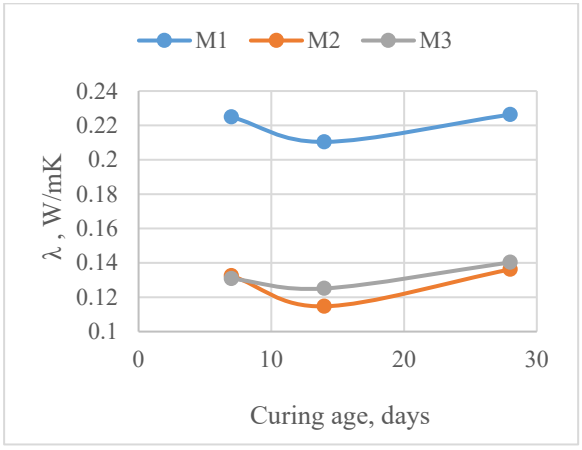

(a)

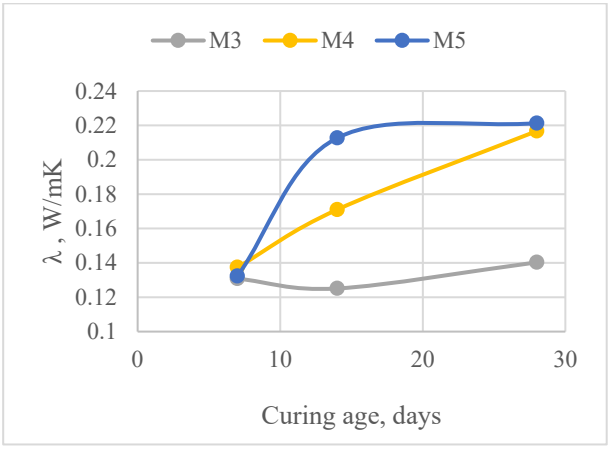

(b)

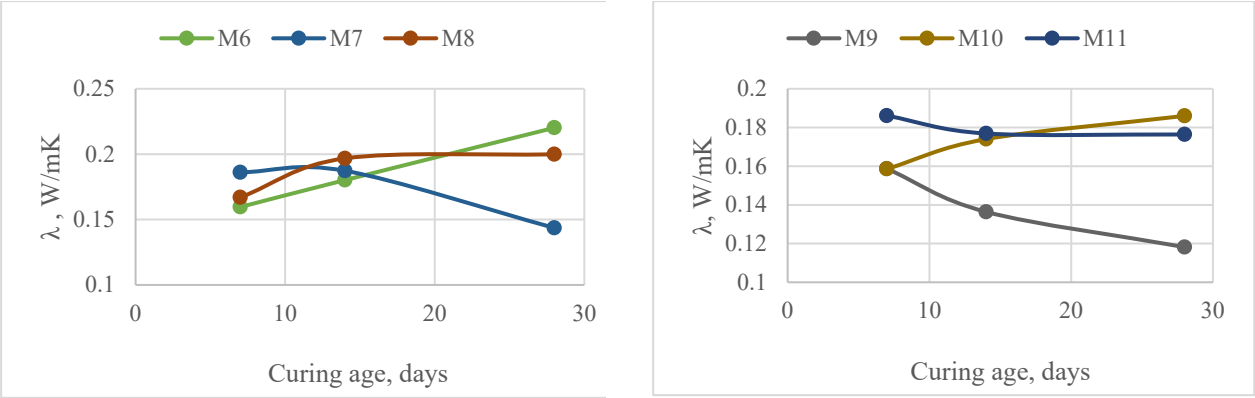

(c) (d)

Figure 4.17. The effect of curing age on thermal conductivity (a) Series 1 (b) Series 2 (c) Series 3 (d) Series 4

4.3.2. Effect of dry density on thermal conductivity

This chapter analyzes the effect of density on thermal conductivity of NAAC. As can be seen from the following figures, mainly as the density increases, thermal conductivity also increases, as the density decreases the thermal conductivity also decreases. This observation coincides with other researchers analysis, in which summarized that the material with lower density will have more pores and larger void spaces between the particles, which are reducing the thermal conductivity of material.

The trend lines of 7 - day and 14 - day cured samples are the same as can be seen in Figure 4.18 and correlation coefficients between density and thermal conductivity R^2 is 74.56% and 58.47%, accordingly. However, the trend line of 28-day cured samples is differ than the 7-day and 14-day cured results; also, the R^2 of 28-day cured results is very low as 0.53% (Figure 4.18-c). Based on the analysis, it was observed that the 28-day cured Mixture 1 had the results, that were out of the range, and thus lead to the opposite trend line demonstration. Therefore, the 28-day cured samples were analyzed again without Mixture 1, and it resulted in higher R^2 value as 46.06% and at the same trend line as the 7-day and 14-day cured results. This result of 28-day cured samples is shown in Figure 4.18-d, where the increase in density leads to the increasing of thermal conductivity.

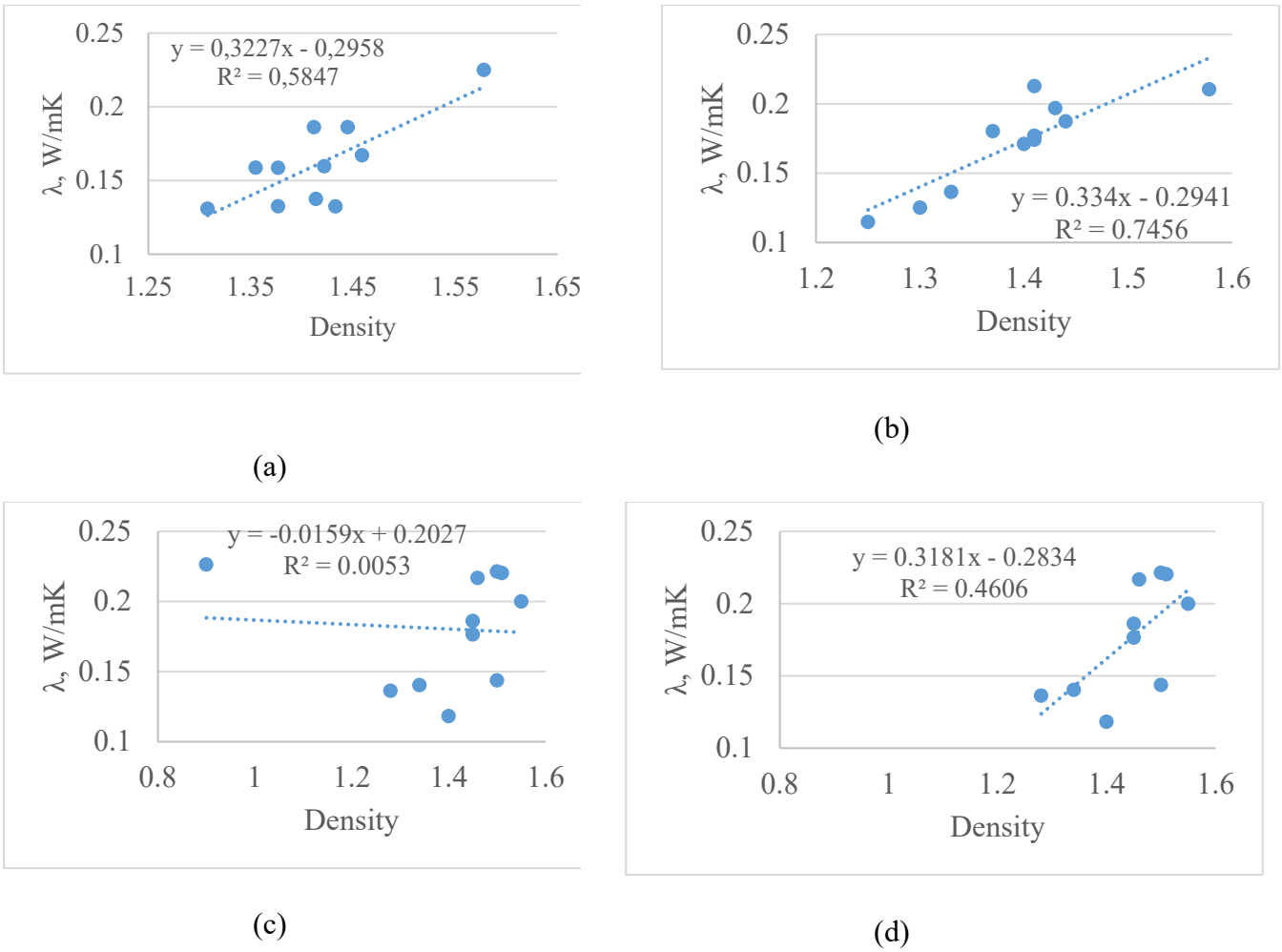

Figure 4.18. Relationship between thermal conductivity and density (a) 7-day cured (b) 14-day cured (c) 28-day cured (d) 28-day cured except M1

Moreover, the relation between density and thermal conductivity was analyzed by series for better determination of dependence between them. According to the Figure 4.19, by series analysis also clearly demonstrated the direct relationship of density and thermal conductivity, because as the density increases, the thermal conductivity also increases in all Series. As can be seen in Table 4.5, in all samples the correlation is higher in Series 1, in which normal sand was replaced with only glass sand, while the correlation between variables was the lowest in samples, containing combined glass sand and glass fiber (Series 3). Because, the addition of glass fiber increases the thermal conductivity as well as density. However, according to test results, the addition of fly ash to the combined samples increases the correlation (Series 4). For examples, in 14-day cured samples the correlation was increased from 54.6% to 99.59% while replacing cement with 30% fly ash. Since, the maximum dependence between density and thermal conductivity observed in 14-day cured samples, these samples would be highlighted as the most success one.

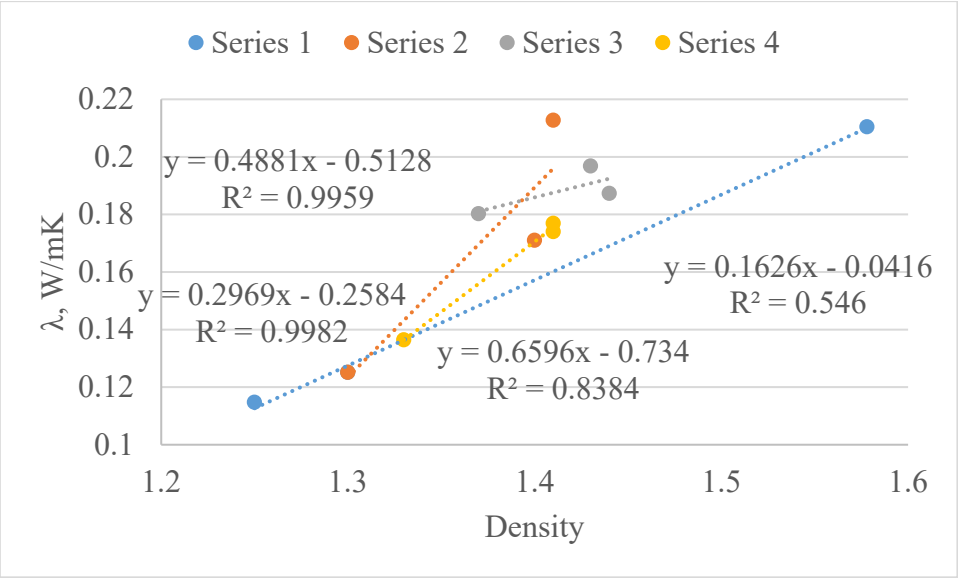

Figure 4.19. Relationship between thermal conductivity and density of 14-day cured samples by series

Table 4.5 Relationship between thermal conductivity and density

	7 day	14 day	28 day
Overall	58,47%	74,56	0,53
Overall (except mixture 1)	21,72%	82,71%	46,06%
Series 1	94,68	99,82	97,26
Series 2	31,94	83,84	96,36
Series 3	16,15	54,6	19,32
Series 4	85,13	99,59	98,29

4.3.3 Effect of porosity on thermal conductivity

This chapter analyzed the effect of porosity on thermal conductivity of NAAC. All sample results, even overall, even by Series show good correlation between the porosity and thermal conductivity. As it was expected, as the porosity increases, the thermal conductivity decreases. Because, a very porous material provides an excellent thermal property [31]. As it was discussed in literature review part, the reaction between aluminum powder, water and calcium hydroxide produces air bubbles, which in case leads to the pore volume increase and generation of voids between particles. Therefore, the porosity is high in NAAC samples and

its increase leads to the improvement of thermal property of NAAC as it was observed in this thesis work results.

The trend line of all mixtures in 7-day, 14-day and 28-day cured samples is approximately the same. As an example, the graph of porosity versus thermal conductivity of 7-day cured samples by overall and by series are shown in Figure 4.20. Moreover, the overall correlation coefficient is higher in 7 day cured samples, which is R^2 = 76.74%. However, the individual analysis by Series shows that in 14-day cured samples the correlation between porosity and thermal conductivity is better (Table 4.6). The maximum and minimum dependence were observed in Series 1 and in Series 3 respectively. It means, the addition of glass fiber weaken the dependence because of the glass fiber, because the glass fiber has a significant effect on the deterioration of thermal property of NAAC.

Table 4.6 Relationship between thermal conductivity and porosity

	7 day	14 day	28 day
Overall	76,74%	57,93	14,92
Series 1	89,92	97,3	96,11
Series 2	58,96	79,14	5,39
Series 3	56,62	67,48	57,82
Series 4	91,98	75,87	97,28

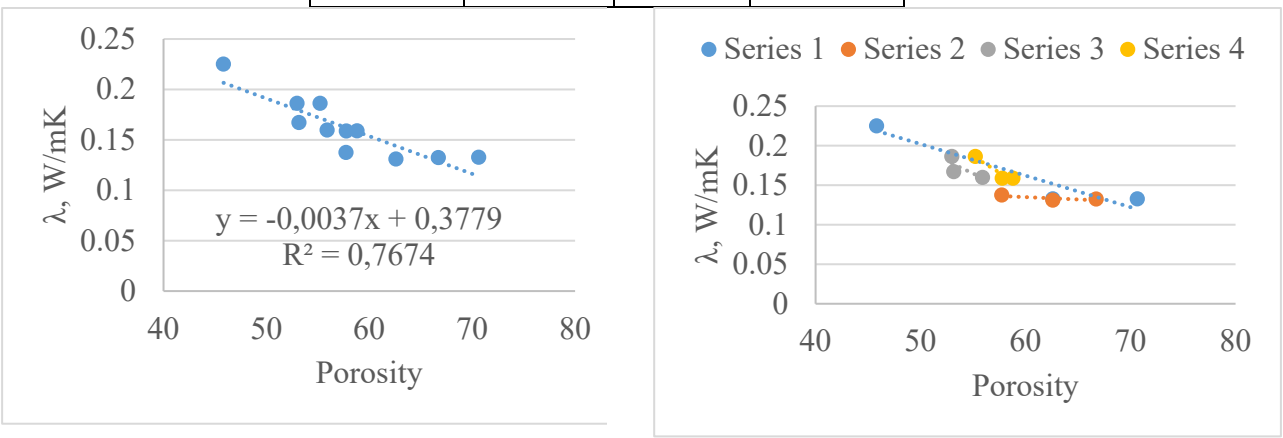

(a) (b)

Figure 4.20. Relationship between thermal conductivity and porosity of 7-day cured samples (a) overall data (b) by series

4.3.4. Effect of water absorption capacity on thermal conductivity

This section analyses the relationship between the absorption and thermal conductivity of NAAC. Based on the results, it was observed that as the absorption increases, the thermal conductivity decreases. Here absorption means the amount of water that penetrates into concrete during the water-curing process. As much water penetrates to NAAC sample, its pore volume increases, which leads to the porosity increase and thus the thermal conductivity will be decreased. Therefore, it can be concluded that the porosity and absorption has the same effect on the thermal characteristics of NAAC. The following Figure 4.21 illustrates the relationship between the absorption and thermal property of 14-day cured samples. As can be seen from both graphs, the overall and by series results show the same trend.

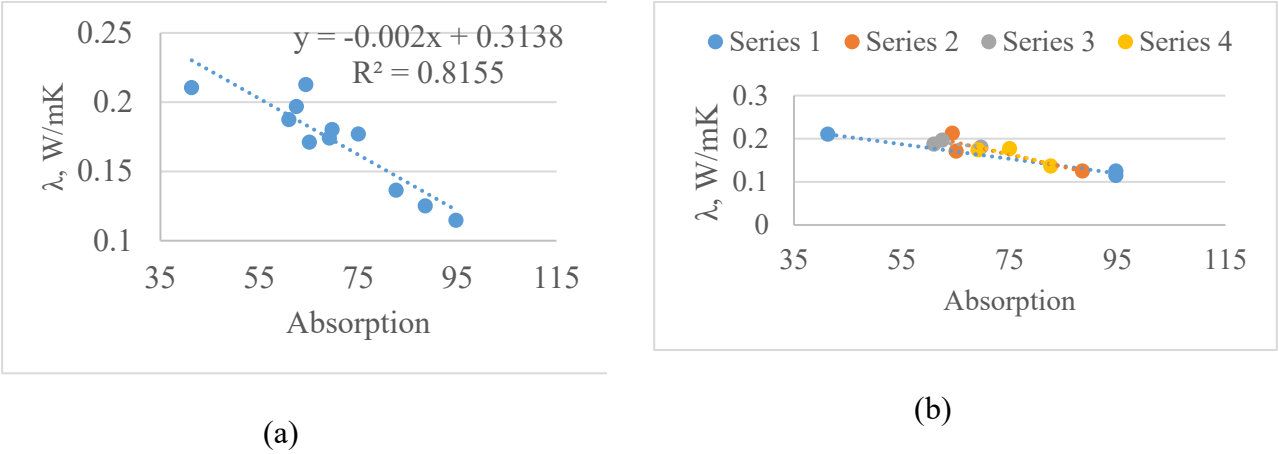

(a) (b)

Figure 4.21. Relationship between thermal conductivity and absorption of 14-day cured samples (a) overall data (b) by series

The following Table 4.7 shows the correlation coefficients between the absorption and thermal conductivity of NAAC. As can be observed, by overall analysis again the 14-day cured samples have the highest R^2, which is 81.55% and 28-day cured samples have the lowest R^2. In Series 1 and in Series 4, the correlation coefficient is high in all day-cured samples, whereas in Series 2 and 3 the 28-day cured samples, the R^2 is lower. It might be explained as the negative effect on long-term periods. Because, the samples were cured longer, and the amount of penetrated water exceeds, thus it leads to the deterioration effect on properties and their relationship.

Table 4.7. Relationship between thermal

conductivity and absorption

	7 day	14 day	28 day
Overall	75,75%	81,55	62,5
Series 1	95,04	99,02	97,65
Series 2	81,91	76,49	46,64
Series 3	100	51,23	47,08
Series 4	86,42	75,87	98,14

4.3.5. Effect of specimen thickness on thermal conductivity

This section investigates the effect of sample thickness on the thermal property. Based on the experimental test results, if the thickness of sample is less, its thermal conductivity is also less and vice versa. The following Figure 4.22 shows this summary in graphic way, in which the increase of thickness leads to the increase of thermal conductivity. Besides, the 14-day and 28-day cured samples, even by series analysis demonstrates the same results with the same trend line, with different R^2 value.

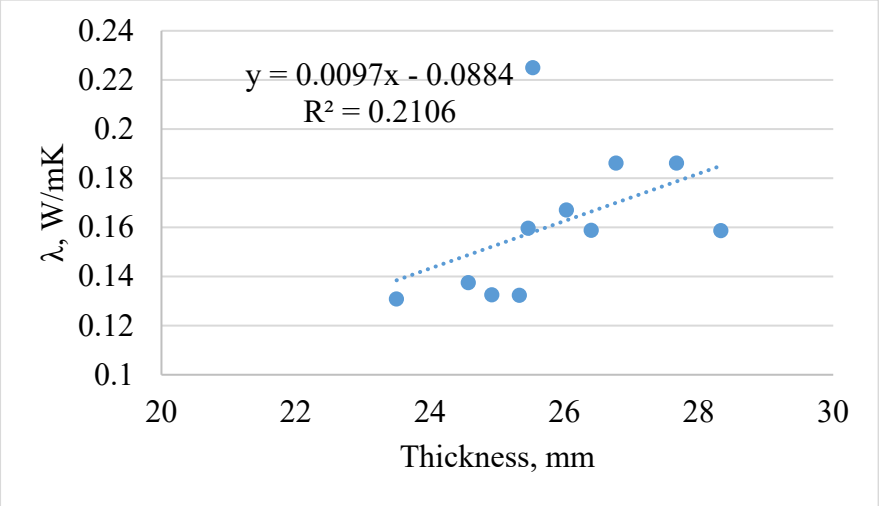

Figure 4.22. Relationship between thermal conductivity and thickness of 7-day cured samples

Chapter 5. Thermal Conductivity Prediction Model, Energy Saving Simulation, and Feasibility of NAAC.

5.1 Energy Saving Simulation: Tool – Design Builder

5.1.1 Geometric aspects of residential building

This part will include the analyzing of energy saving effect of NAAC mixtures using Design Builder software. Design Builder is an energy simulation software, which accurately estimate the energy consumption of building by considering climate of location, envelope and geometry of building, also the thermal characteristics of building materials. In order to analyze the energy saving effect of NAAC mixtures, a five floor residential building was designed, as can be seen in Figure 5.1. The total area of house is 3855 m^2 and area of each floor is 771 m^2.

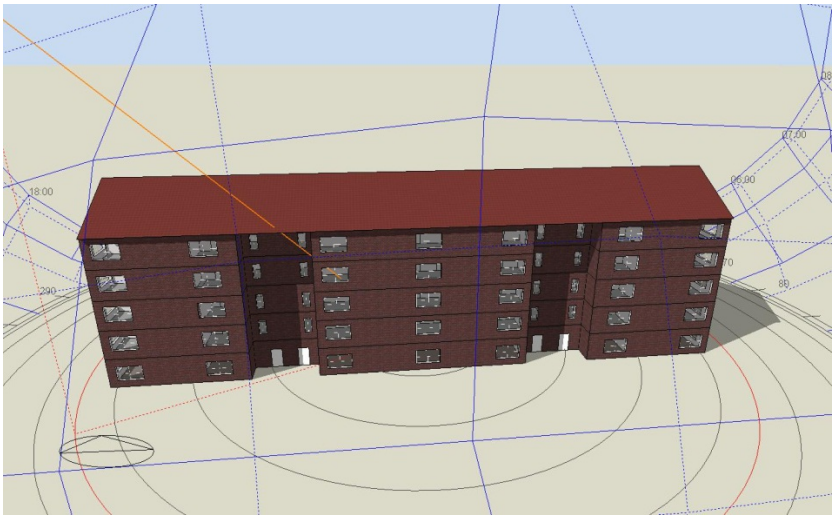

Figure 5. 1. 5-storey residential building model for energy simulation

This residential building consisted of a 1- room, 2-room (base, medium, lux), 3-room and 4-room apartments. The height of each floor is 3 m. Totally, there are fifteen 1-room apartments, fifteen 2-room apartments, five 3-room apartments and five 4-room apartments in this residential house. The characteristics of apartments and area of each room are shown in Table 5.1. As can be seen in Table 5.1, the total area of living quarters in each floor is 542 m2, whereas other 229 m2 was planned for corridor, elevator zone, stairs zone and wheelchair zone.

Table 5.1 Characteristics of apartments.

Rooms	Restroom	Bedroom 1	Bedroom 2	Study zone	Kitchen	Hall	Balcony	WC 1	WC 2	Total Area

										(m2)
4-room apart	28.6	20.5	20.6	18.0	16.9	17.5	9.5	6.2	6.8	144.6
3-room apart	29.1	21.2		15.5	14.3	16.7	9.5	5.7	7.0	119.0
2-room luxe	33.5	21			14.3	5.7	11.1	5.3		91.0
2-room mediu	16.9	14.3			19.0	13.9	5.6	5.8		75.5
2-room base	16.8	15.5			15.5	9.7	5.6	4.1		67.2
1-room apart	16.8				15.6	3.4	5.6	3.4		44.8
Total										**542**

The external wall layer consisted of a decorative plaster, mineral wool, NAAC and cement/plaster/mortar layer. The thickness and other properties of wall layer materials are shown in Table 5.2.

Table 5.2 Properties of wall structure materials

Materials	Thickness (mm)	Thermal conductivity (W/m·K)	Specific heat (J/kg·K)	Density (kg/m^3)	Cost
Decorative Plaster	10	0.33	2040	520	1.26 (GBP/m2)
Mineral Wool	100	0.038	840	140	33.56 (GBP/m3)
NAAC	300	From Experimental Results			25.61 (GBP/m3)
Cement/Plaster/ Mortar	15	0.72	840	1760	0.75 (GBP/m2)

Before starting simulation, the location data, weather data, residential building data, external and internal wall layers, which are main contributes of the energy analysis should be selected as input values. The most important ones are shown in Table 5.3.

Table 5.3 Simulation Input

Location	Uralsk, Kazakhstan
Latitude (°)	51,25
Longitude (°)	51,28
Elevation (m)	37,0

Standard Pressure (kPa)	100,9
ASHRAE climate zone	6A
Koppen classification	Dfb
Residential building	
Occupancy density (people/m2)	0.0385
Heating Setpoint Temperature (°)	18,0
Heating Set Back (°)	12,0
Cooling Setpoint Temperature (°)	25,0
Cooling Set Back (°)	28,0
RH Humidification Setpoint (°)	10,0

Finally, these geometry model and selected material characteristics will be used to assess the energy conservation of residential building with different none-autoclaved aerated concrete material, which consisted of various mixture proportion. Moreover, NAAC wall layer will be compared with another wall structure, which consisted normal concrete panels instead of NAAC. Another wall layer materials and their properties are described in the following Table 5.4. It should be mentioned that the information about cost of materials was taken from local company database. This wall layer consisted of two concrete panels, in which there is a mineral wool between them.

Table 5.4 Concrete wall layer

Materials	Thickness (mm)	Thermal conductivity (W/m·K)	Specific heat (J/kg·K)	Density (kg/m^3)	Cost
Decorative Plaster	10	0,33	2040	520	1,26 (GBP/m2)
External Panel (M400 Concrete)	80	1,2	1000	2400	21,06 (GBP/m3)
Mineral wool (PAROC WAS 35)	180	0,038	840	140	33,56 (GBP/m3)
Internal Panel (M250 Concrete)	140	0,7	1000	2400	17,55 (GBP/m3)
Gypsum/Cement Plaster	15	0,72	840	1760	0,75 (GBP/m2)

5.1.2 Result and Discussion

The following figure 5.2 demonstrates monthly heating and cooling load results of all 11 NAAC mixtures. It should be noted that the 14-day cured NAAC samples were used to

estimate the energy conservation. Because, 14-day cured NAAC samples have the lowest thermal conductivity and highest relationship with physical properties based on the analysis part (Chapter 4). Therefore, the results of all 14-day cured mixtures will be used in this chapter. As can be seen from graphs, the mixture 2 which contains 15% replacement with waste glass sand has the lowest heating and cooling loads in every month, because of the lowest thermal conductivity value. Since the January and July were the coldest and hottest months in a year with the lowest and highest outdoor temperature (Table 5.5), the maximum heating and cooling loads were observed in this months. The mixture 2 records 76391.86 kWh and 10412 kWh of heating and cooling loads respectively at January and July. Compare to batch mixture 1, mixture 2 has the 2.57% and 1.02% lower heating and cooling loads in January and July. Moreover, the greatest heating and cooling loads in every month were observed in mixture 5, which has the highest thermal conductivity value. Thus, it can be summarized, that NAAC mixture with lower λ value will contribute lower heating and cooling loads, than those that have a higher λ value. Therefore, the mixture containing only waste glass sand replacement has the lowest heating and cooling loads in every month, because of the lowest thermal conductivity value. The replacement with 1%, 2% and 3% glass fiber increased the thermal conductivity value, therefore they have more heating and cooling loads than the mixture containing only waste glass sand. However, the heating and cooling load results of combined mixtures (M6, M7, M8) which consisted of both waste glass sand and glass fiber are lower than the batch mixture 1.

Table 5.5 Temperature Data

Temperature (°C)											
Jan.	Feb.	March	Apr.	May	June	July	Aug.	Sept.	Oct.	Nov.	Dec.
-10,6	-10,2	-5,5	5,8	14,2	18,4	20,0	17,6	12,1	5,4	-3,9	-7,7

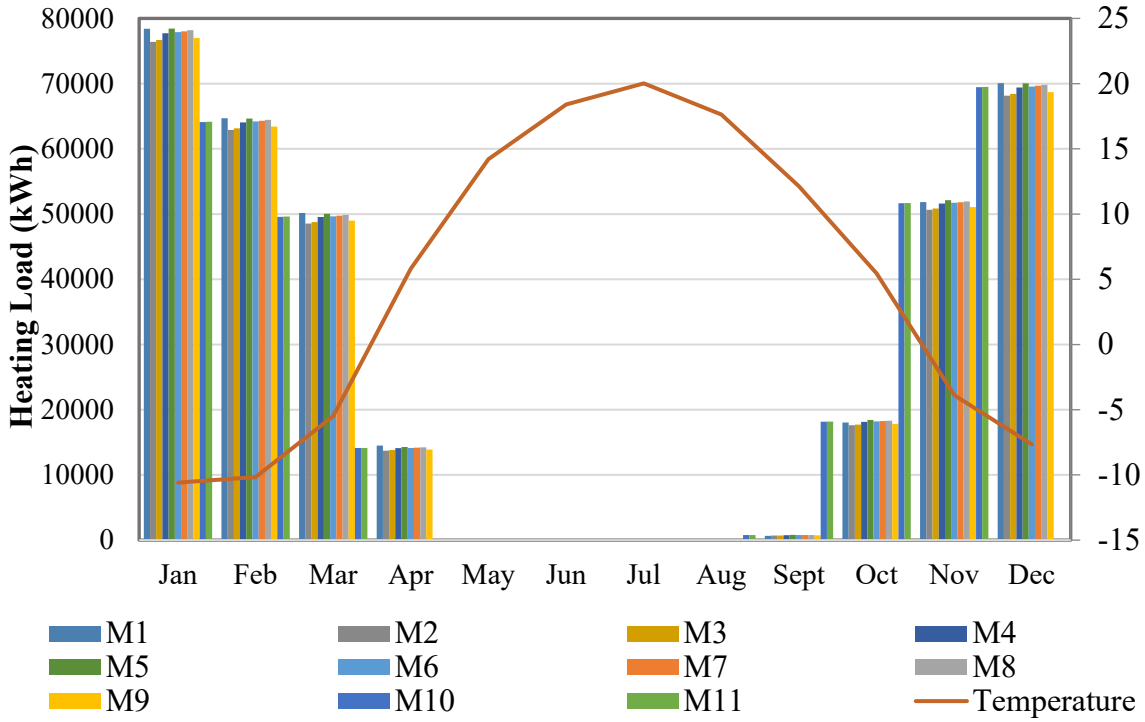

(a)

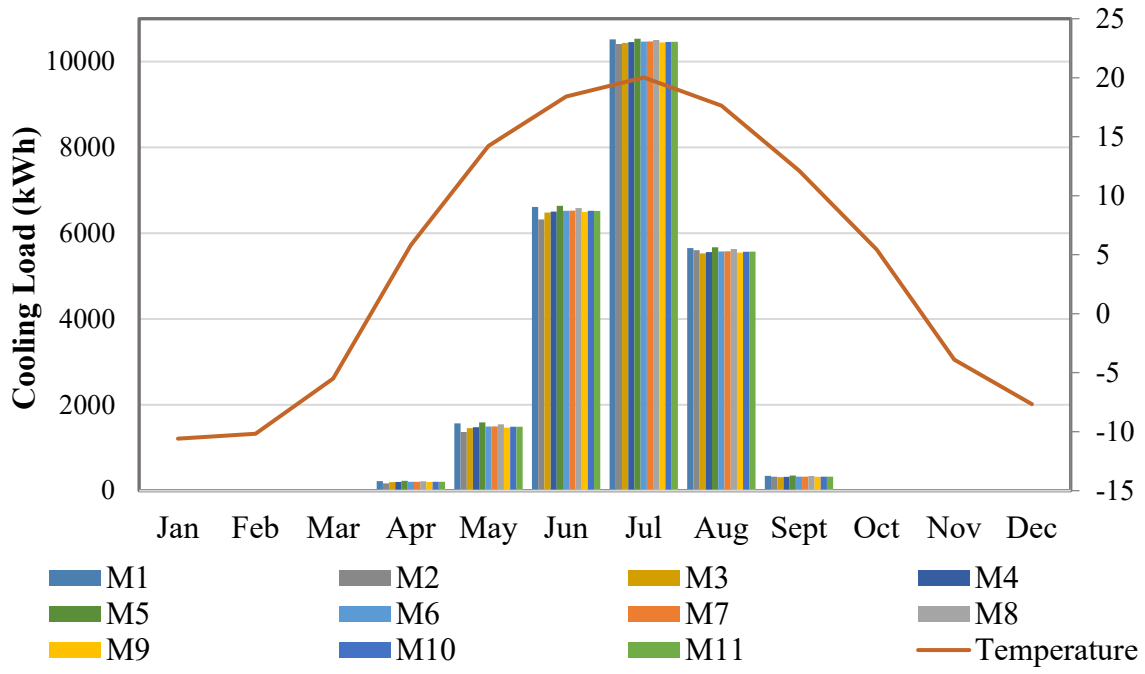

(b)

Figure 5.2. (a). Monthly heating load results, (b) Monthly cooling load results.

The following Table 5.6 shows the annual heating and cooling loads of all mixtures. As can be seen from Table, 15% replacement of normal sand with waste glass sand leads to save 9681 kWh of heating load and 718 kWh of cooling load every year than the batch mixture (M1). The increase of waste glass sand content up to 30% (M3) leads to decrease of

annual heating and cooling load saving to 8203 kWh and 501 kWh respectively. Moreover, the addition of 1%, 2% and 3% glass fiber to the 30% replaced glass sand also leads to save the annual heating load from 0.22 % to 1.93%, and annual cooling load between 0.36% and 1.76% than the batch mixture (M1).

Table 5.6 Annual Heating and Cooling Load Results

Mixt.	Characterization	λ (W/K)	Heating (kWh)	Saving (%)	Cooling (kWh)	Saving (%)
M1	100NS-0WGS-0GF-100C-0FA	0.2104	348357		24924	
M2	85NS-15WGS-0GF-100C-0FA	0.1147	338676	2.78	24206	2.87
M3	70NS-30WGS-0GF-100C-0FA	0.1254	340154	2.35	24423	2.00
M4	70NS-30WGS-0GF-85C-15FA	0.1710	345370	0.86	24526	1.60
M5	70NS-30WGS-0GF-70C-30FA	0.2127	348821	-0.13	25017	-0.37
M6	69.3NS-30WGS-0.7GF-100C-0FA	0.1802	346233	0.61	24596	1.31
M7	68.6NS-30WGS-1.4GF-100C-0FA	0.1873	346825	0.44	24613	1.24
M8	67.9NS-30WGS-2.1GF-100C-0FA	0.1968	347606	0.22	24835	0.36
M9	69.3NS-30WGS-0.7GF-70C-30FA	0.1364	341626	1.93	24485	1.76
M10	68.6NS-30WGS-1.4GF-70C-30FA	0.1740	345651	0.78	24572	1.41
M11	67.9NS-30WGS-2.1GF-70C-30FA	0.1769	345921	0.70	24581	1.37

In the meantime, the following Table 5.7 indicates the simulation results on site and source energy of NAAC materials. This result also shows the effectiveness of mixture 2, which reduces the total site and total source energy down to 6769.58 kWh and 28191.61 kWh because of the lowest thermal conductivity. These values 1.53% and 1.96% lower than the batch mixture. According to the combined mixture parameters, Mixture 9 which contains 30% glass sand, 1% glass fiber and 30% cement saved maximum amount of site and source energy among other combined mixtures (M6 - M12). Therefore, it can be concluded that among NAAC which replaced only with glass sand (M1 – M5), Mixture 2 which contains only 15% glass sand shows the lowest total site and total source energy. Moreover, the combined analysis with glass fiber replacement (M6 – M12), show that Mixture 9, which contains 30% glass sand, 1% glass fiber and 30% fly ash has the lowest total site and source energy. According to the table, it can be concluded that, the increase of glass fiber content leads to increase of thermal conductivity value, which in case leads to the grow up of total site and total source energy.

Table 5.7 Site and Source Energy Results.

Mixt.	Site Energy (kWh)	Saving (%)	Source Energy (kWh)	Saving (%)
M1	441951,37		1439826,96	
M2	435181,79	1.53	1411635,35	1.96
M3	436270,53	1.28	1415997,94	1.65
M4	440145,32	0.4	1431427,23	0.58
M5	442736,82	-0.17	1441666,33	-0.13
M6	440805,19	0.26	1434000,91	0.41
M7	441224,13	0.16	1435729,03	0.28
M8	441814,88	0.03	1438049,840	0.12
M9	437362,03	1.03	1420350,17	1.35
M10	440353,07	0.36	1432258,39	0.53
M11	440556,22	0.32	1433059,8	0.47

Moreover, the energy-saving potential of NAAC wall layer was compared with another wall structure, consisted of two concrete panels, in which there is a mineral wool between them. This type of was layer is considered as the common and most used in construction of houses in Kazakhstan. All information about this wall layer and its properties are given earlier in Table 5.4 and the following Table 5.8 shows the comparison results, in which new wall layer indicated as the Project wall.

Table 5. 8. Comparison between two different wall layer results (annual)

Wall Layers	Heating Load (kWh)	Cooling Load (kWh)	Site Energy (kWh)	Source Energy (kWh)
NAAC M2 wall	338676	24206	435182	1411635
NAAC M9 wall	341626	24485	437362	1420350
Project Wall	339422	24844	435505	1413598

As can be seen from Table 5.8, three different residential wall layer are compared in terms of energy conservation. The first layer NAAC Mixture 2 containing 15% replacement with glass sand and which had the lowest thermal conductivity among other NAAC 11 mixtures. The second layer NAAC Mixture 9 containing combined 30% glass sand and 1% glass fiber and which had the lowest thermal conductivity among the combined mixtures. The third layer is the Project wall, which is commonly used wall layer in construction of residential buildings in Kazakhstan. According to the simulation results, NAAC Mixture 2 will save 746 kWh of heating load and 638 kWh of cooling load annually than the Project wall. The high difference in heating and cooling load between NAAC M2 wall and Project wall was observed in January and in June, approximately because of the maximum and

minimum outdoor temperatures. Moreover, the application of NAAC Mixture 2 in construction of wall layer is also beneficial in terms of site and source energy.

In the meantime, the Project Wall was also compared with NAAC Mixture 9, because Mixture 9 contains combined glass sand and glass fiber. Since, Mixture 9 has a glass fiber in its mixture proportion; its thermal conductivity becomes higher. Therefore, the annual heating load, site energy and source energy of NAAC M9 is 0.65% , 0.43%, 0.48% higher than the Project Wall, respectively. Only in terms of cooling load, NAAC M9 will save 359 kWh annually than the Project Wall based on the simulation results.

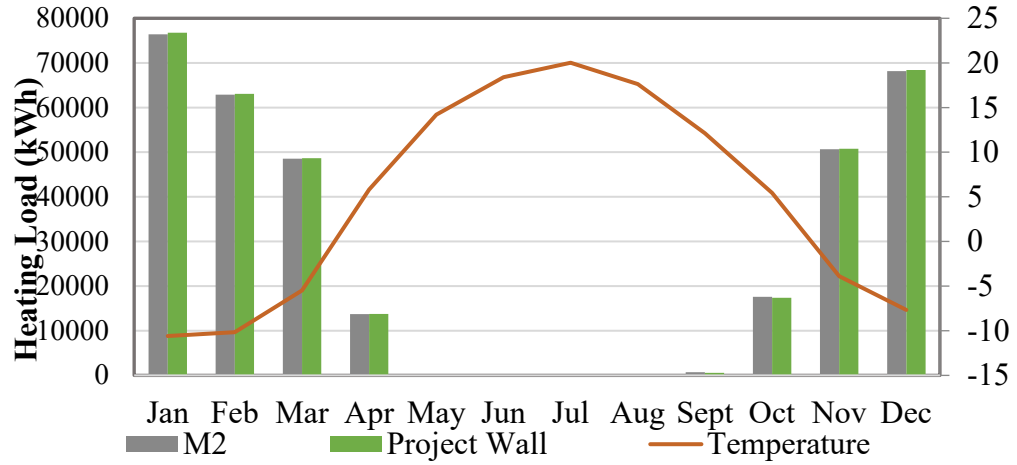

(a)

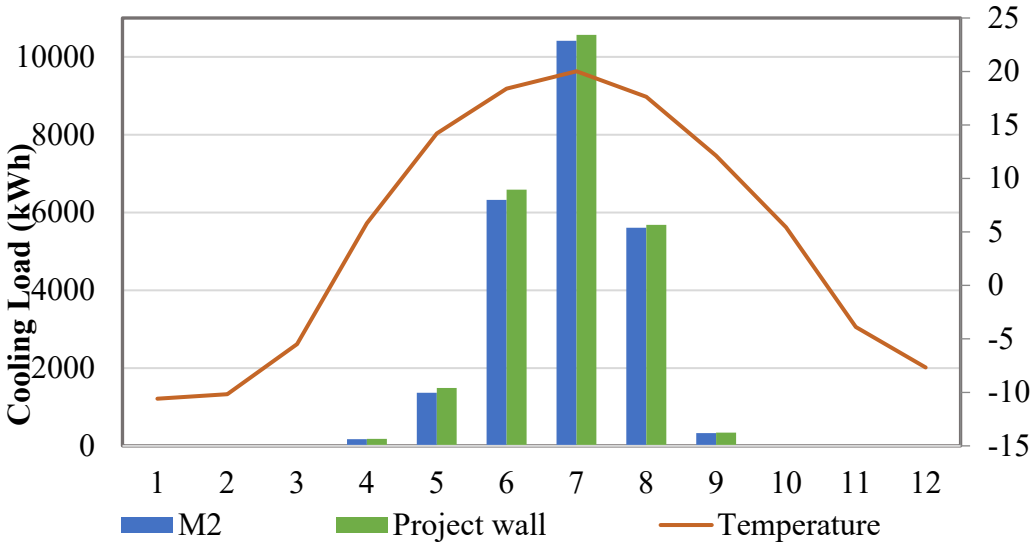

(b)

Figure 5.3. (a) Heating Load of three set wall layer (b) Cooling Load of three set wall layer

According to the comparison, it was observed that NAAC mixture containing only glass sand is beneficial than the Project Wall in terms of energy conservation. However, besides the energy conservation, other mechanical and physical properties should be considered before doing any conclusion in terms of material selection.

5.2 Development of thermal conductivity prediction model based on multi-variable linear regression analysis: Tools-Minitab

The multiple regression analysis (MLR) was conducted in order to predict the equation for thermal conductivity of NAAC. MLR method modeling the equation taking into consideration all physical parameters such porosity, density, thickness, absorption and mixture content parameters such normal sand content, glass sand content, glass fiber, cement and fly ash. Then, the predicted modelling can be used in future estimations of thermal conductivity, which leads to saving of time and laboratory consumables.

The multivariate regression analysis was performed by Excel and Minitab software. In order to show the whole procedure, the 14-day cured sample results were chosen, but the thermal conductivity prediction equation will be developed for all 7-day, 14-day and 28-day cured samples. The following Table 5.9 shows the experimental test results of 14-day cured samples. Thickness (x), density (ρ), porosity (P), absorption (Abs), normal sand (NS), glass sand (GS), glass fiber (GF), cement (C) and fly ash (FA) are considered as the input variables, whereas the thermal conductivity (λ) is the output value.

Table 5.9 Experimental Data for Regression Analysis

Mixt.	λ	x	ρ	P	Abs	NS	GS	GF	C	FA
M1	0,2104	24,74	1,578	45,833	41,31	100	0	0	100	0
M2	0,1147	25,67	1,25	59,96	94,73	85	15	0	100	0
M3	0,1251	25,18	1,3	61,08	88,5	70	30	0	100	0
M4	0,1710	26,27	1,4	54,75	65,1	70	30	0	85	15
M5	0,2127	29,5	1,41	54,59	64,4	70	30	0	70	30
M6	0,1802	30,4	1,37	56,22	69,69	69.3	30	0.7	100	0
M7	0,1873	27,18	1,44	54,17	60,97	68.6	30	1.4	100	0
M8	0,1968	26,33	1,43	54,72	62,51	67.9	30	2.1	100	0
M9	0,1364	30,47	1,33	60,15	82,63	69.3	30	0.7	70	30
M10	0,174	33,5	1,41	57,68	69,15	68.6	30	1.4	70	30

M11	0,1769	33,74	1,41	60,19	75,02	69.3	30	2.1	70	30

The first step of multivariate regression analysis is identification of missing data. Since, it was my own experimental data results, there were no missing data observed. Then, in the second step, the correlation matrix was conducted in order to observe the correlation coefficients between all variables. It was conducted by using Excel Spreadsheet. The variables with highest correlation coefficients are supposed to have the same meaning. Therefore, one of these variables should be eliminated and cannot be included for regression analysis. The following Table 5.10 shows the result of correlation matrix. As can be observed from Table 5.10, mainly absorption is correlated with density and porosity. Moreover, based on the analysis part, where the relation between the absorption and porosity was assessed, it was concluded that the absorption and the porosity has the highest relationship and the same meaning. Therefore, it will be decided whether to eliminate absorption property from the input values or not. Glass sand and normal sand are also have a high correlation, but due to the importance of these variables in prediction of thermal conductivity, it was decided to leave these variables for further analysis. In addition, fly ash and cement also have a high correlation. Because both of them are the cementitious material, which was replaced with each other. However, according to the further analysis, such as p-value it will be decided which one would be included in modelling of thermal conductivity.

Table 5.10 Correlation Matrix

	λ	x	ρ	P	Abs	NS	GS	GF	C	FA
λ		0,1153	0,8635	-0,761	**- 0,903**	0,074	-0,1	0,257	-0,088	0,08769
x			-0,042	0,3943	0,119	-0,512	0,486	0,53	-0,772	0,77195
ρ				-0,878	**-0,971**	0,378	-0,41	0,191	0,0253	-0,0253
P					**0,929**	-0,604	0,6132	0,172	-0,309	0,30928
Abs						-0,333	0,3555	-0,107	-0,099	0,09869
NS							**-0,997**	-0,483	0,3874	-0,3874
GS								0,414	-0,387	0,38666
GF									-0,182	0,18203
C										**-1**

After eliminating most correlated variables, the linearity and normality graphs between input and output variables should be constructed and R^2 value should be identified while proceeding the multiple linear regression analysis. Since, they were already shown in Chapter 4, it was decided to skip them in this chapter. All other steps were performed in Minitab software. As the all variables were inputted to Minitab, software provides the best subset analysis. Best Subset provides the different models and statistics about each model. Then the models can be compared and the best model to predict the thermal conductivity can be chosen. The following Table 5.11 shows the result of Best Subset analysis.

Table 5.11. Simulation Analysis of 14-day cured sample results

#	R^2	Cp	S	Abs	ρ	P	x	NS	C	FA	GS	GF
1	86.2	4.5	0.012215			x		x	x		x	x
2	85	4.8	0.012748	x	x	x	x	x				
3	84.1	6.2	0.013126			x	x	x	x		x	x
4	83.7	6.3	0.13286	x	x	x	x	x			x	x
5	85.8	7.1	0.012393	x	x	x	x	x	x		x	x
6	79.7	8.1	0.014826	x		x	x	x	x	x	x	x
7	80.1	9.0	0.014688	x	x	x	x	x	x	x	x	x

As it shown in Table 5.11, Best Subset analysis provide the 7 different models, more specifically it shows how many and exactly what type of variables should be in equation in order to predict the most precise equation and they will be chosen based on the criteria described below in Table 5.12

Table 5.12. Criteria of Best Subset variables

Statistic variables	Meaning	Criteria
R^2	Exactness coefficient	Higher is better
Cp	Set of terms	Closer to the number of variables
S	Standard error	Lower is better

According to the simulation analysis, the first model has the highest exactness coefficient, which is 86.2% and the lowest standard error, which is 0.012215. Moreover,

there are only five variables, as the porosity, normal sand, glass sand, glass fiber and cement in this model. Furthermore, the model with the second highest exactness coefficient is the model #5. Here the R^2 is 85.8%, which is only lower by 0.04 than the model #1, and the standard error is 0.012393, which is lower by 0.000243 than model #1, also the model #5 contains 8 variables. From my point of view, the difference between the criteria of model #1 and model #5 is so small. Therefore, the model #5, which includes the biggest amount of variables, will be chosen as the best-fit model. Finally, the prediction equation by using eight variables was developed and is shown below in equation 5.1.

$$\boldsymbol{\lambda = -7.06 + 0.0147\,Abs + 1.13\,\rho - 0.0426\,P + 0.00631\,\Delta x + 0.0669\,NS - 0.000263\,Cement + 0.0731\,GS + 0.0771\,GF} \quad \textbf{(5.1)}$$

where,

λ – thermal conductivity, Δ x – thickness, P – porosity, ρ – density, NS – normal sand, GS – glass sand, GF – glass fiber

The same analyses was conducted with 7-day and 28-day cured samples, and their result are shown below in Table 5.13. According to their result, the exactness coefficient is higher and the standard error is lower in 14-day cured samples. Therefore, it can be summarized that the equation 5.1 can be used as a thermal conductivity prediction model of NAAC samples.

Table 5.13. MLR analyses of NAAC samples

	7-day	14-day	28-day
Best-fit model	2,54 + 0,0053 Δx + 0,158 ρ - 0,0053 P + 0,0014 Abs - 0,0251 NS + 0,000015 Cement - 0,0259 GS - 0,0204 GF	$\boldsymbol{\lambda = -7.06 + 0.0147\,Abs + 1.13\,\rho - 0.0426\,P + 0.00631\,\Delta x + 0.0669\,NS - 0.000263\,Cement + 0.0731\,GS + 0.0771\,GF}$	-6,7 - 0,003331 Abs + 0,246 ρ+ 0,00170 P + 0,00203 Δx+ 0,068 NS - 0,000970 Cement + 0,065 GS + 0,046 GF
R^2	70.8 %	85.8%	80.5%
S	0.015742	0.012393	0.017615

5.3. Feasibility of NAAC

This chapter analyzes the feasibility of production and utilization of NAAC in terms of cost. The cost of materials were taken from the database of local company “Bolashak-T”. The following Table 5.14 shows the weight and cost of each material required for $1m^3$ NAAC

production. From various mixture proportions, the mixture 9 was choosen for the cost analysis. Because, mixture 9 comprised of all combined glass sand and glass fiber. Moreover, based on the energy analysis, this mixture summarized as the energy efficient than the other combined mixtures. Finally, the cost of materials needed to produce 1m^3 NAAC is 51.45 $. In addition, the exchange rate from Dollar ($) to Tenge (KZT) is assumed to be 433.

Table 5.14. The cost of materials for 1 m3 of NAAC.

№	Material	Mass, kg/1 m3 of NAAC	Cost, tg/kg	Total cost, tg
1	Sand	395	1.15	454.25
2	Cement	363	16	5808
3	Water	533	0.271	144.4
4	Lime	247	14	3458
5	Aluminum powder	2.97	615	1826.55
6	Gypsum	120	28	3360
7	Glass sand	184	22	4048
8	Glass fiber	4.45	470	2091.5
9	Fly ash	121	9	1089
For 1 m3 NAAC				**22279.74 KZT**
				51.45 $

The following Table 5.15 presents the machinersy cost. All materials shown in Table 5.14 are assumed as ready materials, except glass sand. Thereofore, the next step is to estimate the cost of glass sand and NAAC samples production. The jaw crusher and ball mill machinery will be used to grind the glass and preparing the glass sand, whereas the mixer will be used to prepare the NAAC samples. Based on the analysis, the machinery cost to prepare 1 m3 NAAC was estimeated as the 3.8 $. The cost analysis also includes the electricity cost of all machine, as shown in Table 5.16. Here, the electricity cost for 1 kWh is assumed to be 0.0405$. Therefore, the total electricity cost was estimated as the 6.243 $. Moreover, the workers salary was estimated as the 5.54 $ for 1m3 production of NAAC. All information about the salary of workers and the workload per day were taken form the local factory, that produce the construction materials.

Table 5.15. Machinery cost.

№	Machinery	Cost, $	Lifetime production, tons	Material weight, tons / 1 m^3 of NAAC	Cost of production, $/1 m3 of NAAC
1	Jaw crusher	2800	6240	0.184	0.0826
2	Ball mill	10000	8320	0.184	0.0221
3	Concrete mixer	10523	5616	1.97	3.69

For 1 m3 NAAC	**3.8 $**

Table 5.16. Electricity cost

№	Equipment	Electricity per ton, kWh	Material weight, tons / 1 m^3 of NAAC	Electricity cost, $/1 m3 of NAAC
1	Jaw crusher	1.833	0.184	0.337
2	Ball mill	9.250	0.184	0.069
3	Concrete mixer	2.963	1.97	5.837
For 1 m3 NAAC				**6.243 $**

Table 5.17. Salary for workers

№	Equipment	# of workers	Salary of workers, $/day	Workload, t/day	Material weight, tons / 1 m^3 of NAAC	Total salary, $
1	Jaw crusher	1	10	0.8	0.184	0.8
2	Ball mill	1	10	0.8	0.184	0.8
3	Concrete mixer	2	10	5	1.97	3.94
For 1 m3 NAAC						**5.54$**

Finally, the total cost of materials and production of 1 m^3 NAAC comprised as 51.45 $ and 15.583 $, respecrively. So, based on the feasibility analysis, total cost of 1m^3 NAAC comprised of combined glass sand and glass fiber is 67$. These cost is slightly higher than the conventional materials in Kazakhstan, because of the use of glass fiber. However, the money can be saved from the utility bills every year, since the developed NAAC will perform better mechanical and thermal characteristics than those conventional materials.

Chapter 6. Conclusion

The purpose of thesis was to analyze the combined effect of waste glass sand and glass fiber on the thermal properties of NAAC. To obtain this goal, the mixture proportion of NAAC consisting of combined glass sand and glass fiber were developed. Then, the integrated experimental works were conducted in order to prepare sample and evaluate its properties. The main part of this study was to analyze all test results and indicate the relationship between mechanical, physical and thermal properties of NAAC. In addition, the thermal performance of developed NAAC samples were simulated by Design Builder software. Finally, the statistical model to predict the thermal conductivity of NAAC was conducted by Minitab Software. After successful completion of all mentioned tasks, the conclusion and recommendations will be discussed in this part.

Firstly, the major findings of test result analysis part are summarized as the followings:

- The increase of glass aggregate content leads to decrease the thermal conductivity.
- The increase of fly ash content leads to increase the thermal conductivity of NAAC.
- The increase of glass fiber content leads to increase the thermal conductivity of NAAC.
- The thermal conductivity of the NAAC mixture combined with soda-lime glass sand and glass fiber was lower than that of the NAAC mixture containing normal sand.
- The decrease of curing age leads to decrease the thermal conductivity of NAAC.
- The lower value of density leads to the lower thermal conductivity.
- The increase of porosity leads to decrease the thermal conductivity.
- The increase of absorption leads to decrease the thermal conductivity
- The thicker sample will have a higher thermal conductivity than the thinner one.
- The increase of glass sand content leads to increase the compressive strength.
- The combined use of glass sand with glass fiber has a synergetic effect on compressive and flexural strength.

- The increase of ultrasonic pulse velocity also leads to increase the compressive strength.
- The increase in porosity and water absorption leads to decrease the density of NAAC.

Another conclusion was made in terms of energy saving effect of materials. NAAC mixture with lower λ value will contribute lower heating and cooling loads, than those that have a higher λ value. Therefore, the mixture 2 containing 15% glass sand has the lowest heating loads, cooling loads, total site and source energy in every month because of the lowest thermal conductivity value among other mixtures. The comparison with common used wall material also verified the efficiency of NAAC Mixture 2 in terms of energy consumption. It can be summarized that the NAAC Mixture 2 with the lowest thermal conductivity value provides better thermal insulation, conserves temperature, reduces energy consumption, and reduces utility bills for heating /cooling the house.

In addition, the developed mixture parameters and test results were suitable to predict the thermal conductivity equation with the 85.5% exactness. Moreover, the feasibility analysis show that the total cost (materials + production) of 1 m3 NAAC was slightly higher than the other conventional materials in Kazakhstan, because of the glass fiber use. However, the money can be saved from the utility bills, since the developed NAAC performs better mechanical and thermal characteristics.

To sum up, several recommendations can be summarized as the followings:

- The long-term effect of combined glass sand and glass fiber on the thermal properties of NAAC should be analyzed.
- The Alkali – Silica Reaction between the aggregate and cementitious materials should be analyzed, since it has a deleterious effect on concrete behavior.
- More measurements (more mixture parameters) are needed in order to precisely predict the model based on the Multivariate Linear Regression analysis.

Reference

[1] Narayanan N, Ramamurthy K. 2000. “Structure and properties of aerated concrete: a review”. Cement Concrete Composites 22 (5): 321–29.

[2] Hamad, Ali j., 2014. “Materials, Production, Properties and Application of Aerated Lightweight Concrete: Review,” International Journal of Materials Science and Engineering 2(2): 152-157.

[3] Kim, K-H., Jeon, S-E., Kim, J-K., Yang, S., 2002. “An experimental study on thermal conductivity of concrete”, Cement and Concrete Research 33: 363-371

[4] Cary, V., Doolitle, K., Lin, S., Lizardo, D., Marzen, S., 2014. “High Strength Non Autoclaved Aerated Concrete”. Retrieved 9.02.2020 from http://web.mit.edu/dlizardo/www/3402_report.pdf

[5] Jiang, Yi, Tung-Chai Ling, Kim Hung Mo, and Caijun Shi. 2019. "A critical review of waste glass powder–Multiple roles of utilization in cement-based materials and construction products." Journal of Environmental Management 242: 440-449.

[6] Karazi, S. M., I. U. Ahad, and K. Y. Benyounis. 2017. "Laser Micromachining for Transparent Materials."

[7] Tengri News. 2018. “New life of bottle or how to make money on glass” Received from https://tengrinews.kz/fotoarchive/1048/

[8] Clean Household Energy Consumption in Kazakhstan: A Roadmap. 2020. Retrieved 11.01.2021 from https://www.iea.org/reports/clean-household-energy-consumption-in-kazakhstan-a-roadmap

[9] Drochytka, Rostislav, Jiří Zach, Azra Korjenic, and Jitka Hroudová. "Improving the energy efficiency in buildings while reducing the waste using autoclaved aerated concrete made from power industry waste." Energy and Buildings 58 (2013): 319-323.

[10] Coradini, E. (2009). Green Material v. Legislation: Autoclaved Aerated Concrete Faces an Uphill Fight in California. Environmental Design & Construction. 12(9), 38.

[11] European Autoclaved Aerated Concrete Association. 2018. Energy Efficiency. Retrieved 21.01.2019 from https://www.eaaca.org/index.php/aac/energy-efficiency

[12] Radhi, H. (2008). A Systematic Methodology for Optimizing the Energy Performance of Building in Bahrain. Energy and Buildings. 40(7), 1297-1301.

[13] HULYA AYBEK. 2013. ENERGY PERFORMANCE EVALUATION OF AAC. Retrieved 18.02.2019 from http://www.mhsl.uab.edu/dt/2013/Aybek_uab_0005D_11014.pdf

[14] Kaska, O., & Yumrutas, R. (2008). Comparison of Experimental and Theoretical Result for the Transient Heat Flow through Multilayer Walls and Flat Roofs. Energy. 33(12), 1816-1823.

[15] Heathcote, K. (2007). Comparison of the Summer Thermal Performance of Three Test Buildings that Predicted by the Admittance Procedure. Architectural Science Review. 51(1), 31-38.

[16] Arizona State University, College of Engineering and Applied Sciences. (2007). A Comparison of Innovative Exterior Wall Construction Techniques. pp. 9, 34. Mesa: AZ. Sawhney, A., & Mund, A.

[17] Liu, Yiwei, Caijun Shi, Zuhua Zhang, and Ning Li. 2019. "An overview on the reuse of waste glasses in alkali-activated materials." *Resources, Conservation and Recycling* 144: 297-309.

[18] Liang, Hong, Huiying Zhu, and Ewan A. Byars. 2007. "Use of waste glass as aggregate in concrete." In *7th UK CARE Annual General Meeting. UK Chinese Association of Resources and Environment, Greenwich*, vol. 15.

[19] Pehlivanlı, Zühtü Onur, İbrahim Uzun, Zeynep Pınar Yücel, and İlhami Demir. 2016. "The effect of different fiber reinforcement on the thermal and mechanical properties of autoclaved aerated concrete." *Construction and Building Materials* 112: 325-330.

[20] Gautam, S. P., Srivastava, V., & Agarwal, V. C. 2012. Use of glass wastes as fine aggregate in Concrete. *J. Acad. Indus. Res,* 1(6), 320-322.

[21] Dong, Z., Sun, Q., & Zhang, W. (2020). Thermal and physical properties of concrete containing glass after cooling in different paths. *Structural Concrete,* 21(3), 1071-1081.

[22] Chung, S. Y., Abd Elrahman, M., Sikora, P., Rucinska, T., Horszczaruk, E., & Stephan, D. 2017. Evaluation of the effects of crushed and expanded waste glass aggregates on the material properties of lightweight concrete using image-based approaches. *Materials,* 10(12), 1354.

[23] Yu, R.; van Onna, D.V.; Spiesz, P.; Yu, Q.L.; Brouwers, H.J.H. Development of ultra-lightweight fibre reinforced concrete applying expanded waste glass. J. Clean. Prod. 2016, 112, 690–701.

[24] Alani, A.; MacMullen, J.; Telik, O.; Zhang, Z.Y. Investigation into the thermal performance of recycled glass screed for construction purposes. Const. Build. Mater. 2012, 29, 527–532.

[25] Swamy, R.N. 2003. The alkali-silica reaction in concrete. 2 nd edn., USA: Taylor and Francis, p.335.

[26] ASTM International, 2003, “Standard Specification for Concrete Aggregates”, C 33-03.

[27] Wirth, K., and Barth, A., 2017, “X-Ray Fluorescence (XRF)”, Macalester College, Indiana University and Purdue University, Indianapolis, USA.

[28] ASTM International, 2016, “Standard Test Method for Compressive Strength of Hydraulic Cement Mortars”, C 109 – 16.

[29] ASTM International, 2016, “Standard Test Method for Flexural Strength of Hydraulic Cement Mortars”, C 348-02.

[30] ASTM International, 2016, “Standard Test Method for Pulse velocity Through Concrete”, C 597-02.

[31] Shabbar, Rana, Paul Nedwell, and Zhangjian Wu. 2018. "Porosity and Water Absorption of Aerated Concrete with Varying Aluminium Powder Content." Int. J. Eng. Technol 10, no. 3.

[32] Schober, Georg. 2011. "Porosity in autoclaved aerated concrete (AAC): A review on pore structure, types of porosity, measurement methods and effects of porosity on

properties." In 5th International Conference on Autoclaved Aerated Concrete, no. 39–43, pp. 351-359. Bydgoscsz Poland.

[33]. Design Builder.2020. “For Energy Assessors”. Received from https://designbuilder.co.uk/simulation

[34] Eskin, Nurdil, and Hamdi Türkmen. 2008. "Analysis of annual heating and cooling energy requirements for office buildings in different climates in Turkey." Energy and Buildings 40, no. 5: 763-773.

[35] Fathalian, Afshin, and Hadi Kargarsharifabad. 2018. "Actual validation of energy simulation and investigation of energy management strategies (Case Study: An office building in Semnan, Iran)." Case studies in thermal engineering 12: 510-516.

[36] Joe, Jaewan, Wonjun Choi, Hansol Kwon, and Jung-ho Huh. 2013. "Load characteristics and operation strategies of building integrated with multi-story double skin facade." Energy and buildings 60: 185-198.

[37] Z.S. Zomorodian, M. Tahsildoost. 2016. “Validation of energy simulation programs: an empirical and comparative approach, Iran.” Journal of Energy 18 (4) 115–132.

[38] Sadeghifam, Aidin Nobahar, Seyed Mojib Zahraee, Mahdi Moharrami Meynagh, and Iman Kiani. 2015. "Combined use of design of experiment and dynamic building simulation in assessment of energy efficiency in tropical residential buildings." Energy and Buildings 86: 525-533.

[39] Pawar, B.S. and Kanade, G.N., 2018. Energy Optimization of Building Using Design Builder Software. International Journal of New Technology and Research, 4(1), p.263152.

[40] Cárdenas, J., G. Osma, C. Caicedo, A. Torres, S. Sánchez, and G. Ordóñez. 2016. "Building energy analysis of Electrical Engineering Building from DesignBuilder tool: calibration and simulations." In IOP Conference Series: Materials Science and Engineering, vol. 138, no. 1, p. 012013. IOP Publishing.

[41] Overview for Multiple Regression. 2020. “Support Minitab”. Received from https://support.minitab.com/en-us/minitab-express/1/help-and-how-to/modeling-statistics/regression/how-to/multiple-regression/before-you-start/overview/

[42] Jerome, Lawrence. 2009. "Multiple linear and non-linear regression in Minitab." RATIO 1: 0-0005.

[43] Obianyo, Ifeyinwa Ijeoma, Esther Nneka Anosike-Francis, Gina Odochi Ihekweme, Yang Geng, Ruoyu Jin, Azikiwe Peter Onwualu, and Alfred BO Soboyejo. "Multivariate regression models for predicting the compressive strength of bone ash stabilized lateritic soil for sustainable building." 2020. Construction and Building Materials 263: 120677.

[44] Sakar, E., Sıddık Keskin, and H. Unver. "Using of factor analysis scores in multiple linear regression model for prediction of kernel weight in Ankara walnuts." J. Anim. Plant Sci 21, no. 2 (2011): 182-185.

[45] Al-Ghandoor, A., and M. Samhouri. 2009. "Electricity consumption in the industrial sector of Jordan: application of multivariate linear regression and adaptive neuro-fuzzy techniques." JJMIE 3, no. 1: 69-76.

[46] Anderson, Michael D., Khalid Sharfi, and Sampson E. Gholston. 2006. "Direct demand forecasting model for small urban communities using multiple linear regression." Transportation research record (1): 114-117.

Appendices

Appendix A

Table A1. The density of thermal conductivity specimens

	Density overall			**Density by series**			
	7-day cured	14-day cured	28-day cured	7-day cured	14-day cured	28-day cured	
M1	1,578	1,578	0,9				
M2	1,377	1,25	1,28	1,421	1,376	1,173	**Series 1**
M3	1,308	1,3	1,34				
M4	1,414	1,4	1,46				
M5	1,433	1,41	1,5	1,385	1,37	1,433	**Series 2**
M6	1,422	1,37	1,51				
M7	1,445	1,44	1,5				
M8	1,459	1,43	1,55	1,442	1,413	1,52	**Series 3**
M9	1,355	1,33	1,4				
M10	1,377	1,41	1,45				
M11	1,412	1,41	1,45	1,381	1,383	1,433	**Series 4**
AVE	**1,4164**	**1,3935**	**1,3945**				

Table A2. The porosity of thermal conductivity specimens

	Porosity Overall			**Porosity by Series**			
M1	7-day cured	14-day cured	28-day cured	7-day cured	14-day cured	28-day cured	
M2	45,833	45,833	60,52				
M3	70,651	59,96	59,19	59,70	55,62	59,54	**Series 1**
M4	62,609	61,08	58,92				
M5	57,754	54,75	56,94				
M6	66,736	54,59	62,78	62,37	56,81	59,55	**Series 2**
M7	55,913	56,22	60,9				
M8	52,997	54,17	64,66				
M9	53,174	54,72	58,01	54,03	55,04	61,19	**Series 3**
M10	58,82	60,15	65,9				
M11	57,785	57,68	58,99				
	55,231	60,19	58,71	57,28	59,34	61,20	**Series 4**
AVE	**57,955**	**56,304**	**60,502**				

Table A3. The absorption of thermal conductivity specimens

	Absorption Overall			**Absorption by series**			
M1	7-day cured	14-day cured	28-day cured	7-day cured	14-day cured	28-day cured	
M2	41,31	41,31	43,36				
M3	106,14	94,73	86,89	79,82	74,85	69,42	**Series 1**
M4	92	88,5	78,01				
M5	70,67	65,1	64,47				
M6	88,13	64,4	74,17	83,60	72,67	72,22	**Series 2**
M7	65,47	69,69	68,58				
M8	58	60,97	76,41				
M9	57,94	62,51	59,82	60,47	64,39	68,27	**Series 3**
M10	77,37	82,63	89,51				
M11	72,52	69,15	68,57				
	64,25	75,02	68,43	71,38	75,60	75,50	**Series 4**
AVE	**72,163636**	**70,36454545**	**70,7472727**				

Appendix B

Table B1. The compressive strength and physical properties results of 7-day cured samples

7-day cured Mixtures	Compressive Strength (MPa)	Absorption (%)	Bulk Density (g/cm3)	Porosity (%)	D/P
M1	0,434	86,7	1,28	59,38	0,022
M2	0,747	107,82	1,39	71,75	0,019
M3	0,919	73,25	1,36	57,54	0,024
M4	1,295	58,61	1,53	56,61	0,027
M5	0,798	78	1,46	63,64	0,023
M6	1,851	58,74	1,51	55,77	0,027
M7	2,35	50,11	1,53	50,95	0,030
M8	3,892	41,72	1,56	46,02	0,034
M9	1,708	59,3	1,46	53,85	0,027
M10	1,914	59,7	1,46	54,58	0,027
M11	1,94	60,06	1,46	54,60	0,027

Table B2. The compressive strength and physical properties results of 14-day cured samples

Mixtures	Compressive Strength (MPa)	Absorption (%)	Bulk Density (g/cm3)	Porosity (%)	D/P
M1	0,311	93,55	1,34	64,89	0,021
M2	0,843	82,4	1,32	59,66	0,022
M3	1,083	72,71	1,38	58,06	0,024
M4	1,695	56,25	1,51	54,35	0,028
M5	0,945	65,92	1,44	56,86	0,025
M6	1,96	60,86	1,49	56,19	0,027
M7	2,069	56,6	1,52	54,87	0,028
M8	4,074	42,91	1,58	47,46	0,033
M9	2,359	53,92	1,52	52,89	0,029
M10	2,259	56,52	1,5	54,07	0,028
M11	1,84	67,52	1,46	58,72	0,025

Table B3. The compressive strength and physical properties results of 28-day cured samples

Mixtures	Compressive Strength (Mpa)	Absorption (%)	Bulk Density (g/cm3)	Porosity (%)	D/P
M1	0,403	96,84	1,33	65,08	0,0204
M2	0,891	82,68	1,35	60,96	0,0221
M3	1,26	77,07	1,36	59,3	0,0229

M4	1,766	57,37	1,54	56,12	0,0274
M5	1,702	68,97	1,51	61,22	0,0247
M6	2,258	63,73	1,54	60,07	0,0256
M7	2,71	50,11	1,53	50,95	0,03
M8	5,189	42,18	1,58	46,81	0,0338
M9	1,768	75,01	1,46	62,23	0,0235
M10	3,496	54,03	1,48	51,8	0,0286
M11	3,498	59,98	1,47	55,15	0,0267

Table B4. The flexural strength and physical properties results of 7-day cured samples

Mixtures	Flexural Strength (MPa)	Absorption (%)	Bulk Density (g/cm3)	Porosity (%)	D/P
M1	1,047	58,17	1,55	56,76	0,02731
M2	0,816	108,09	1,22	63,36	0,01926
M3	1,903	84,39	1,34	60,92	0,022
M4	1,394	50,96	1,54	52,05	0,02959
M5	1,943	91,47	1,3	61,9	0,021
M6	1,593	64,17	1,47	57,18	0,02571
M7	1,469	51,88	1,56	53,08	0,02939
M8	1,502	59,82	1,49	55,45	0,02687
M9	2,006	65,72	1,47	58,21	0,02525
M10	1,735	61,72	1,49	56,62	0,02632
M11	1,88	64,32	1,49	58,10	0,02565

Table B5. The flexural strength and physical properties results of 14-day cured samples

Mixtures	Flexural Strength (Mpa)	Absorption (%)	Bulk Density (g/cm3)	Porosity (%)	D/P
M1	1,047	58,17	1,55	56,76	0,02731
M2	0,816	108,09	1,22	63,36	0,01926
M3	1,903	84,39	1,34	60,92	0,022
M4	1,394	50,96	1,54	52,05	0,02959
M5	1,943	91,47	1,3	61,9	0,021
M6	1,593	64,17	1,47	57,18	0,02571
M7	1,469	51,88	1,56	53,08	0,02939
M8	1,502	59,82	1,49	55,45	0,02687
M9	2,006	65,72	1,47	58,21	0,02525
M10	1,735	61,72	1,49	56,62	0,02632
M11	1,88	64,32	1,49	58,10	0,02565

Table B6. The flexural strength and physical properties results of 28-day cured samples

Mixtures	Flexural Strength (Mpa)	Absorption (%)	Bulk Density (g/cm3)	Porosity (%)	D/P
M1	1	61,66	1,52	57,78	0,02631
M2	1,894	48,82	1,35	43,59	0,03097
M3	1,643	89,31	1,31	61,37	0,02135
M4	1,611	52,91	1,57	54,1	0,02902
M5	0,563	99,73	1,35	67,54	0,01999
M6	1,531	65,88	1,54	60,81	0,02532
M7	1,615	56	1,51	54,11	0,02791
M8	2,152	56,51	1,58	56,83	0,0278
M9	1,919	68,93	1,49	60,55	0,02461
M10	1,801	63,5	1,48	57,42	0,02577
M11	1,883	55,96	1,51	54,27	0,02782